

Smooth μ -Hybrid and Non-Minimal Higgs Inflation in $SU(4)_C \times SU(2)_L \times SU(2)_R$ With Observable Gravitational Waves

Umer Zubair

Department of Physics and Astronomy,
University of Delaware, Newark, DE 19716, USA

E-mail: umer@udel.edu

Abstract. We propose to study a smooth variant of the μ -hybrid inflation model and a non-minimal Higgs model of inflation with quartic non-minimal coupling between the Higgs field and gravity within the context of a realistic GUT gauge group based on supersymmetric $SU(4)_C \times SU(2)_L \times SU(2)_R$. These models are incorporated with a realistic scenario of reheating and non-thermal leptogenesis, compatible with the constraints from the baryon asymmetry of the universe. Notably, both models successfully address the MSSM μ -problem and avoid the issue of primordial magnetic monopoles. Our analysis reveals that both models predict a scalar spectral index n_s that closely aligns with the central observationally favored value of Planck2018 + BICEP2/Keck Array (BK15) data and yield a large tensor-to-scalar ratio ($r > 10^{-3}$), potentially detectable in forthcoming CMB experiments.

Contents

1	Introduction	1
2	The SUSY $SU(4)_C \times SU(2)_L \times SU(2)_R$ Model	3
3	Smooth μ-Hybrid Inflation	6
3.1	MSSM μ -Term	9
3.2	Reheating and Non-Thermal Leptogenesis	10
3.3	Inflationary Observables	12
3.4	Inflationary Predictions and Comparison with Observations	13
4	Non-Minimal Higgs Inflation	17
4.1	MSSM μ -Term	19
4.2	Reheating and Non-Thermal Leptogenesis	21
4.3	Inflationary Observables	22
4.4	Inflationary Predictions and Comparison with Observations	23
5	Observable Primordial Gravitational Waves	27
6	Proton Decay	28
7	Summary	28

1 Introduction

Observations thus far have confirmed several key predictions of the most basic inflationary models. These include a spectrum that is nearly, though not precisely, scale-invariant, consisting of predominantly Gaussian and adiabatic scalar perturbations [1]. Within the framework of inflationary theory, the mechanism driving the formation of cosmic structures may also generate a significant background of primordial gravitational waves (PGWs). These waves, referred to as tensor perturbations, imprint their signature on the polarization of the Cosmic Microwave Background (CMB) [2], offering a potential avenue for observation using present-day technology [3–5]. A detection of the tensor signal would offer unprecedented insight into the earliest epochs of our Universe, bolstering the case for large-field inflation and offering profound implications for our comprehension of the inflationary period and physics at extremely high energies [6].

Given that the energy scale of inflation closely aligns with SUSY gauge unification, SUSY hybrid inflation [7–14] naturally integrates into grand unified theories, with the GUT scale M_{GUT} providing the correct order of magnitude for the amplitude of primordial scalar fluctuations [7]. Thus, supersymmetric hybrid inflation serves as an excellent

framework for bridging inflationary cosmology with particle physics at the GUT scale. On the other hand, there is also a compelling temptation to incorporate Higgs inflation into SUSY grand unified theories within a supergravity framework.

In the minimal SUSY hybrid inflation model [8, 13, 14], inflation ends abruptly, transitioning into a ‘waterfall’ phase where undesirable topological defects, such as magnetic monopoles, can arise [15] if predicted by the GUT gauge group, potentially leading to cosmological catastrophes. To address this issue, various extensions to inflation models have been proposed, including shifted hybrid inflation [16–18], smooth hybrid inflation [19–21], and new inflation [22–25]. Among these, the smooth hybrid inflation model stands out for several reasons. Unlike standard and shifted hybrid inflation, the potential of smooth hybrid inflation possesses a slope at the classical level, driving inflation without the need for radiative corrections. Moreover, the system follows a specific valley of minima, leading to a particular point on the vacuum manifold, thereby preventing the formation of topological defects at the end of inflation, a feature shared also by shifted hybrid inflation.

The non-minimal Higgs inflation [26, 27] emerges from a non-minimal coupling between the Inflaton Higgs field and the Ricci scalar, \mathcal{R} . The GUT gauge group spontaneously breaks during inflation due to the non-zero values acquired by the relevant Higgs superfields, thereby avoiding the problem of primordial magnetic monopoles. Additionally, akin to the smooth hybrid inflation model, the potential in non-minimal Higgs inflation exhibits inclination at the tree-level, obviating the necessity for radiative corrections.

The Pati-Salam symmetry G_{422} exhibits numerous remarkable features and is an attractive choice for a grand unified theory (GUT). It provides a natural framework for implementing the leptogenesis scenario due to the presence of right-handed neutrinos, leading to tiny but non-zero neutrino masses through the seesaw mechanism. Furthermore, it facilitates third-family Yukawa unification (YU) [28–33], charge quantization, and avoids the doublet-triplet splitting problem since both Higgs doublets are contained in a bi-doublet rather than the GUT scale Higgs fields. The combination of third-family Yukawa unification with non-universalities in the gaugino or the scalar sector can be made consistent with low-energy phenomenology. For the amelioration of the little hierarchy problem in G_{422} model with the help of non-universal gaugino masses at the GUT scale, see [34]. Additionally, due to the $U(1)_R$ symmetry, various dangerous proton decay operators are effectively suppressed. The unbroken $\mathbb{Z}_2^{\text{mp}} \subset U(1)_R$ acts as matter parity, implying the existence of a stable lightest supersymmetric particle (LSP) and thus a potential dark matter candidate.

In this paper, we introduce the smooth μ -hybrid inflation model for the first time, employing the mechanism proposed in [35] for generating the MSSM μ -term in combination with smooth hybrid inflation. This model is embedded in a realistic GUT based on $SU(4)_C \times SU(2)_L \times SU(2)_R$ gauge symmetry and possesses several notable features. It naturally avoids the magnetic monopole problem, generates the MSSM μ -term, and does not require radiative corrections due to the inclination present at the tree level. This is in contrast to the shifted μ -hybrid inflation [36, 37], where one-loop radiative

corrections play an important role in driving inflation. Additionally, using the same superpotential, we study a non-minimal Higgs inflation model by employing a special form of Kahler potential [38], resulting in a quartic non-minimal coupling of the inflaton Higgs field to gravity. In this setup, the conjugate Higgs fields assume the role of the inflaton, driving inflation. Both models incorporate a realistic scenario of reheating and non-thermal leptogenesis consistent with the constraints from the observed baryon asymmetry of the universe (BAO). The predictions of both models for the scalar spectral index n_s are in accordance with the Planck2018 + BICEP2/Keck Array (BK15) data [1], and they readily accommodate observable values of the tensor-to-scalar ratio r , which can be probed by a variety of forthcoming CMB experiments. Lastly, the proton decay rate is heavily suppressed to have any observable signature in the next generation of experiments, rendering it practically stable.

The remainder of the paper is structured as follows: Section 2 presents an overview of the supersymmetric $SU(4)_C \times SU(2)_L \times SU(2)_R$ model. Section 3 delves into the implementation of smooth μ hybrid inflation, along with a discussion on the inflationary predictions and their comparison with observational data. Section 4 focuses on the implementation of the non-minimal Higgs inflation model, presenting results, predictions and their comparison with observations. The potential detection of observable primordial gravitational waves in upcoming experiments is briefly addressed in Section 5, while Section 6 provides a brief discussion on proton decay. Finally, the findings are summarized in Section 7.

2 The SUSY $SU(4)_C \times SU(2)_L \times SU(2)_R$ Model

The SUSY Pati-Salam (PS) model is based on the gauge symmetry $G_{422} = SU(4)_C \times SU(2)_L \times SU(2)_R$. The MSSM matter superfields, including the right handed neutrino, reside in the following irreducible representations of G_{422} [39],

$$\begin{aligned} F_i &= (\mathbf{4}, \mathbf{2}, \mathbf{1}) \equiv \begin{pmatrix} u_{ir} & u_{ig} & u_{ib} & v_{il} \\ d_{ir} & d_{ig} & d_{ib} & e_{il} \end{pmatrix}, \\ F_i^c &= (\bar{\mathbf{4}}, \mathbf{1}, \mathbf{2}) \equiv \begin{pmatrix} u_{ir}^c & u_{ig}^c & u_{ib}^c & v_{il}^c \\ d_{ir}^c & d_{ig}^c & d_{ib}^c & e_{il}^c \end{pmatrix}, \end{aligned} \quad (2.1)$$

where $i = 1, 2, 3$ denotes the family index and the subscripts r, g, b, l denote the four colors of $SU(4)_C$. The model unifies each family of quarks and leptons into above two representations. Note that F and F^c comprise the $\mathbf{16}$ (spinorial) representation of $SO(10)$: $\mathbf{16} \rightarrow F(\mathbf{4}, \mathbf{2}, \mathbf{1}) + F^c(\bar{\mathbf{4}}, \mathbf{1}, \mathbf{2})$.

The Higgs sector of G_{422} consists of the following superfields: (i) a pair of GUT

Higgs superfields H^c and \bar{H}^c represented as,

$$\begin{aligned} H^c &= (\bar{\mathbf{4}}, \mathbf{1}, \mathbf{2}) \equiv \begin{pmatrix} u_{Hr}^c & u_{Hg}^c & u_{Hb}^c & v_{Hl}^c \\ d_{Hr}^c & d_{Hg}^c & d_{Hb}^c & e_{Hl}^c \end{pmatrix}, \\ \bar{H}^c &= (\mathbf{4}, \mathbf{1}, \mathbf{2}) \equiv \begin{pmatrix} \bar{u}_{Hr}^c & \bar{u}_{Hg}^c & \bar{u}_{Hb}^c & \bar{v}_{Hl}^c \\ \bar{d}_{Hr}^c & \bar{d}_{Hg}^c & \bar{d}_{Hb}^c & \bar{e}_{Hl}^c \end{pmatrix}, \end{aligned} \quad (2.2)$$

which trigger the spontaneous breaking of G_{422} gauge symmetry to G_{SM} by acquiring nonzero vacuum expectation values (VEVs) along the right-handed sneutrino directions ($|\langle v_{Hl}^c \rangle| = |\langle \bar{v}_{Hl}^c \rangle| = M$) with the following symmetry breaking pattern

$$SU(4)_C \times SU(2)_L \times SU(2)_R \xrightarrow[M]{\langle H^c, \bar{H}^c \rangle} SU(3)_C \times SU(2)_L \times U(1)_Y;$$

(ii) a bi-doublet Higgs superfield h represented as,

$$h = (\mathbf{1}, \mathbf{2}, \mathbf{2}) \equiv (h_u \ h_d) = \begin{pmatrix} h_u^+ & h_d^0 \\ h_u^0 & h_d^- \end{pmatrix}, \quad (2.3)$$

which, after the G_{422} symmetry breaking, splits into electroweak Higgs doublets h_u and h_d whose neutral components subsequently develop VEVs $\langle h_u \rangle = v_u$, $\langle h_d \rangle = v_d$ with $\tan \beta = v_d/v_u$; (iii) a sextet Higgs superfield $G = (\mathbf{6}, \mathbf{1}, \mathbf{1})$, which after G_{422} symmetry breaking, splits into two color-triplet Higgs superfields g, g^c providing superheavy masses to the color-triplet pair d_H^c and \bar{d}_H^c ; (iv) and finally, a gauge singlet superfield $S = (\mathbf{1}, \mathbf{1}, \mathbf{1})$ whose scalar component acts as an inflaton. The bi-doublet h and the sextet G comprise the $\mathbf{10}$ representation of $SO(10)$: $\mathbf{10} \rightarrow h(\mathbf{1}, \mathbf{2}, \mathbf{2}) + G(\mathbf{6}, \mathbf{1}, \mathbf{1})$. The decomposition of the above G_{422} representations under the SM gauge group, along with their global $U(1)_R$ and Z_2 charges, is given in Table 1.

The superpotential of the model consistent with the $U(1)_R$ and G_{422} symmetries is given by [40]

$$\begin{aligned} W &= \kappa S \left(M_*^2 - \frac{(\bar{H}^c H^c)^2}{m_P^2} \right) + \lambda S h^2 \\ &+ \gamma^{ij} F_i^c F_j h + a G H^c H^c + b G \bar{H}^c \bar{H}^c \\ &+ \frac{\bar{H}^c \bar{H}^c}{m_P} \left(\alpha_1^{ij} F_i^c F_j^c + \alpha_2^{ij} F_i F_j \right) + \frac{H^c H^c}{m_P} \left(\beta_1^{ij} F_i^c F_j^c + \beta_2^{ij} F_i F_j \right), \end{aligned} \quad (2.4)$$

where $\kappa, \lambda, \gamma^{ij}, \alpha_{1,2}^{ij}, \beta_{1,2}^{ij}, a$ and b are real and positive dimensionless couplings and M_* is a super heavy mass scale. The UV cutoff m_P (reduced Planck mass) has replaced the cutoff Λ [20] typically employed in smooth hybrid inflation models [19], which controls the non-renormalizable terms in the superpotential. The global $U(1)_R$ symmetry plays

G_{422} REPRESENTATIONS	GLOBAL SYMMETRIES		DECOMPOSITION UNDER G_{SM}
	$U(1)_R$	\mathbb{Z}_2	
MATTER SECTOR			
$F_i (\mathbf{4}, \mathbf{2}, \mathbf{1})$	1	1	$Q_i (\mathbf{3}, \mathbf{2}, 1/6)$ $L_i (\mathbf{1}, \mathbf{2}, -1/2)$
$F_i^c (\bar{\mathbf{4}}, \mathbf{1}, \mathbf{2})$	1	1	$u_i^c (\bar{\mathbf{3}}, \mathbf{1}, -2/3)$ $d_i^c (\bar{\mathbf{3}}, \mathbf{1}, 1/3)$ $\nu_i^c (\mathbf{1}, \mathbf{1}, 0)$ $e_i^c (\mathbf{1}, \mathbf{1}, 1)$
HIGGS SECTOR			
$H^c (\bar{\mathbf{4}}, \mathbf{1}, \mathbf{2})$	0	1	$u_H^c (\bar{\mathbf{3}}, \mathbf{1}, -2/3)$ $d_H^c (\bar{\mathbf{3}}, \mathbf{1}, 1/3)$ $\nu_H^c (\mathbf{1}, \mathbf{1}, 0)$ $e_H^c (\mathbf{1}, \mathbf{1}, 1)$
$\bar{H}^c (\mathbf{4}, \mathbf{1}, \mathbf{2})$	0	-1	$\bar{u}_H^c (\mathbf{3}, \mathbf{1}, 2/3)$ $\bar{d}_H^c (\mathbf{3}, \mathbf{1}, -1/3)$ $\bar{\nu}_H^c (\mathbf{1}, \mathbf{1}, 0)$ $\bar{e}_H^c (\mathbf{1}, \mathbf{1}, -1)$
$h (\mathbf{1}, \mathbf{2}, \mathbf{2})$	0	1	$h_u (\mathbf{1}, \mathbf{2}, 1/2)$ $h_d (\mathbf{1}, \mathbf{2}, -1/2)$
$G (\mathbf{6}, \mathbf{1}, \mathbf{1})$	2	1	$g (\mathbf{3}, \mathbf{1}, -1/3)$ $g^c (\bar{\mathbf{3}}, \mathbf{1}, 1/3)$
$S (\mathbf{1}, \mathbf{1}, \mathbf{1})$	2	1	$S (\mathbf{1}, \mathbf{1}, 0)$

Table 1: The representations of matter and Higgs superfields under G_{422} gauge symmetry, their decomposition under G_{SM} along with their global $U(1)_R$ and \mathbb{Z}_2 charges.

essential role in realizing successful inflation. It ensures the linearity of superpotential W in S , forbidding non-linear terms which could spoil inflation [7]. Its unbroken \mathbb{Z}_2^{mp} subgroup acts as ‘matter parity’, which implies a stable LSP, thereby making it a plausible dark matter candidate. Finally, it forbids several dangerous proton decay operators. The superpotential in (2.4) respects an additional discrete \mathbb{Z}_2 symmetry under which the combination $H^c \bar{H}^c$ is odd, and therefore, only even powers of the combination $H^c \bar{H}^c$

are allowed. All other fields are neutral under this \mathbb{Z}_2 symmetry. Note that the terms $(H^c)^4$ and $(\bar{H}^c)^4$ can also appear in the superpotential but become irrelevant in the D -flat direction.

The first two terms in the first line of the superpotential (2.4) are pertinent to smooth hybrid inflation, while the third term $(\lambda S h_u h_d)$ gives rise to the effective μ -term, derived below. The first term in the second line encompasses the Yukawa couplings, providing masses to quarks and leptons following electroweak symmetry breaking. The last two terms, involving the sextuplet superfield G , yield superheavy masses for the color-triplets d_H^c and \bar{d}_H^c . The terms in the third line are relevant for proton decay while the term with coupling α_1^{ij} yields heavy right-handed neutrino masses for the see-saw mechanism.

3 Smooth μ -Hybrid Inflation

The superpotential terms relevant for smooth μ -hybrid inflation are

$$W \supset \kappa S \left(M_*^2 - \frac{(\bar{H}^c H^c)^2}{m_P^2} \right) + \lambda S h^2, \quad (3.1)$$

where h^2 denotes the unique bilinear invariant $\epsilon_{ij} h_u^i h_d^j$. The global SUSY scalar potential obtained from the above superpotential is given by

$$\begin{aligned} V = & \kappa^2 \left| M_*^2 - \frac{(\bar{H}^c H^c)^2}{m_P^2} + \frac{\lambda}{\kappa} h^2 \right|^2 + 4\lambda^2 h^2 |S|^2 \\ & + \frac{4\kappa^2 |S|^2 |\bar{H}^c|^2 |H^c|^2}{m_P^4} \left(|\bar{H}^c|^2 + |H^c|^2 \right) + D\text{-terms}, \end{aligned} \quad (3.2)$$

where the scalar components of the superfields are denoted by the same symbols as the corresponding superfields. The VEV's of the fields at the global SUSY minimum of the above potential are given by,

$$\langle S \rangle = 0, \quad \langle h \rangle = 0, \quad \langle \bar{H}^c H^c \rangle = M^2 = M_* m_P. \quad (3.3)$$

The D -flatness condition yields $\bar{H}^{c*} = e^{i\theta} H^c$ and $h_{ui} = e^{i\phi} \epsilon_{ij} h_d^{j*}$, where θ and ϕ are arbitrary phases. Restricting ourselves to the direction with $\theta = 0$ ($\bar{H}^c = H^c$), which contains the smooth inflationary path and the SUSY vacua, as well as stabilizing the potential at $h = 0$, we obtain,

$$V = \kappa^2 M_*^4 \left[\left(1 - \frac{|H^c|^4}{M^4} \right)^2 + 8 \frac{|S|^2 |H^c|^6}{M^8} \right], \quad (3.4)$$

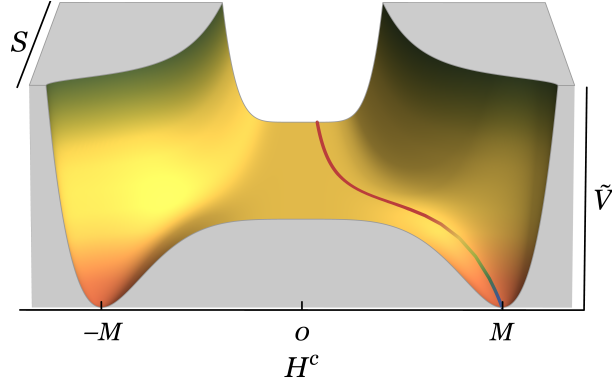


Figure 1: The tree-level, global SUSY scalar potential ($\tilde{V} = V/V_0$) features two symmetric valleys of local minima that can serve as inflationary trajectories. These valleys, while not classically flat, already exhibit an inclination at the tree level, can drive the inflaton towards the SUSY vacua. Unlike standard SUSY or shifted hybrid inflation scenarios, there is no need for radiative corrections, which typically contribute subdominantly to the slope of the inflationary trajectories.

The above scalar potential can be written in terms of the dimensionless variables

$$y = \frac{|H^c|}{M}, \quad z = \frac{|S|}{M}, \quad (3.5)$$

as follows,

$$V = V_0 \left(\left(1 - y^4\right)^2 + 8z^2 y^6 \right), \quad (3.6)$$

where $V_0 = \kappa^2 M_*^4$ and $M = \sqrt{M_* m_P}$. The potential is displayed in Figure 1 which shows two valleys of minima, approximated in the large z limit as

$$y_{\pm}(z) = \pm \left(\sqrt{1 + 9z^4} - 3z^2 \right)^{1/2} \simeq \pm \frac{1}{\sqrt{6}z}. \quad (3.7)$$

This valley of local minimum is not flat and possess a slope that drives the inflaton towards the SUSY vacuum. Along the inflationary trajectory, SUSY is broken due to the presence of a non-zero vacuum energy density $V_0 = \kappa^2 M_*^4$, which in turn generates radiative corrections. These radiative corrections, however, are expected to have a negligible effect on the inflationary predictions, and therefore, we can safely ignore these contributions in our numerical calculations. Furthermore, along this inflationary trajectory ($y = y_+, z \gg 1$), the G_{422} gauge symmetry breaks during inflation, and the potentially catastrophic magnetic monopoles resulting from the breaking of both $SU(4)_C$ and $SU(2)_R$ symmetries are effectively inflated away.

Assuming gravity-mediated SUSY breaking [41, 42], where SUSY is broken in the hidden sector and is communicated gravitationally to the observable sector, the soft

potential is [43]

$$V_{\text{Soft}} = M_{\varphi_i}^2 |\varphi_i|^2 + m_{3/2} (\varphi_i W_i + (A - 3) W + h.c.), \quad (3.8)$$

where φ_i is observable sector field, $W_i = \partial W / \partial \varphi_i$, $m_{3/2}$ is the gravitino mass and A is the complex coefficient of the trilinear soft SUSY-breaking terms. The effective contributions of soft SUSY breaking terms during inflation can be written as,

$$V_{\text{Soft}} = a m_{3/2} \kappa M_*^2 |S| + M_S^2 |S|^2 = a m_{3/2} \kappa M_*^2 M z + M_S^2 M^2 z^2, \quad (3.9)$$

with

$$a = 2|A - 2| \cos(\arg S + \arg |A - 2|),$$

where a and M_S are the coefficients of soft SUSY breaking linear and mass terms for S , respectively. Here, we assume appropriate initial conditions for $\arg S$ so that a remains constant during inflation [13, 44]. For the impact of $\arg S$ on the inflationary dynamics in standard hybrid inflation, see [45].

To describe physics near the Planck scale, it is crucial to incorporate supergravity (SUGRA) corrections, as they have an important effect on the global SUSY potential.

The non-minimal Kähler potential may be expanded as

$$\begin{aligned} K = & K_M + \kappa_S \frac{|S|^4}{4m_P^2} + \kappa_{H^c} \frac{|H^c|^4}{4m_P^2} + \kappa_{\bar{H}^c} \frac{|\bar{H}^c|^4}{4m_P^2} + \kappa_h \frac{|h|^4}{4m_P^2} \\ & + \kappa_{SH^c} \frac{|S|^2 |H^c|^2}{m_P^2} + \kappa_{S\bar{H}^c} \frac{|S|^2 |\bar{H}^c|^2}{m_P^2} + \kappa_{Sh} \frac{|S|^2 |h|^2}{m_P^2} \\ & + \kappa_{H^c \bar{H}^c} \frac{|H^c|^2 |\bar{H}^c|^2}{m_P^2} + \kappa_{H^c h} \frac{|H^c|^2 |h|^2}{m_P^2} + \kappa_{\bar{H}^c h} \frac{|\bar{H}^c|^2 |h|^2}{m_P^2} \\ & + \kappa_{SS} \frac{|S|^6}{6m_P^4} + \dots, \end{aligned} \quad (3.10)$$

where K_M is the minimal Kähler potential and is given as

$$K_M = |S|^2 + |H^c|^2 + |\bar{H}^c|^2 + |h|^2. \quad (3.11)$$

The F -term SUGRA scalar potential is given by

$$V_{\text{SUGRA}} = e^{K/m_P^2} \left(K_{i\bar{j}}^{-1} D_{\varphi_i} W D_{\varphi_j^*} W^* - 3m_P^{-2} |W|^2 \right), \quad (3.12)$$

with φ_i being the bosonic components of the superfields $\varphi_i \in \{S, H^c, \bar{H}^c, h, \dots\}$, and we have defined

$$D_{\varphi_i} W \equiv \frac{\partial W}{\partial \varphi_i} + m_P^{-2} \frac{\partial K}{\partial \varphi_i} W, \quad K_{i\bar{j}} \equiv \frac{\partial^2 K}{\partial \varphi_i \partial \varphi_j^*}, \quad (3.13)$$

and $D_{\varphi_i}^* W^* = (D_{\varphi_i} W)^*$. The SUGRA scalar potential during inflation becomes

$$V_{\text{SUGRA}} = V_0 \left(1 - \frac{1}{54z^4} + \left(\frac{8+3\kappa_S}{54z^2} - \kappa_S z^2 \right) \left(\frac{M}{m_p} \right)^2 + \left(\frac{1-4\kappa_S+6\gamma_S z^4}{12} \right) \left(\frac{M}{m_p} \right)^4 + \dots \right). \quad (3.14)$$

Putting soft SUSY breaking mass terms and SUGRA corrections together, we obtain the following form of inflationary potential,

$$\begin{aligned} V &\simeq V_{\text{SUGRA}} + V_{\text{Soft}} \\ &\simeq V_0 \left(1 - \frac{1}{54z^4} + \left(\frac{8+3\kappa_S}{54z^2} - \kappa_S z^2 \right) \left(\frac{M}{m_p} \right)^2 + \left(\frac{1-4\kappa_S+6\gamma_S z^4}{12} \right) \left(\frac{M}{m_p} \right)^4 + \frac{a m_{3/2} M}{M_*^2} z + \frac{M_S^2 M^2}{M_*^4} z^2 \right), \end{aligned} \quad (3.15)$$

where $\gamma_S = 1 - \frac{7\kappa_S}{2} + 2\kappa_S^2 - 3\kappa_{SS}$ and we have retained terms up to $O((|S|/m_p)^4)$ from SUGRA corrections. The dominant contribution to the potential arises solely from the terms involving higher powers of S as all other fields ($|H^c| \sim (M/|S|)M$) are significantly suppressed in comparison ($|S| \gg M$).

The inclusion of supergravity corrections often leads to the so called η problem [8] by generating a large inflaton mass, which could spoil inflation. In the case of SUSY hybrid inflation with a minimal Kähler potential, as a direct consequence of $U(1)_R$ symmetry, a cancellation of the mass squared term through the interplay of the exponential factor and other part of the potential naturally circumvents this problem. On the other hand, for a non-minimal Kähler potential, this mass squared term appears with a coupling κ_S which can be tuned ($\kappa_S \lesssim 0.01$) to ensure adequate flatness of the potential, required for successful inflation.

3.1 MSSM μ -Term

The MSSM μ -term within the framework of the smooth hybrid inflation model can be derived as follows. The SUSY potential (3.2) in the D -flat direction, combined with the soft mass terms from Eq. (3.9), is given by:

$$\begin{aligned} V_{\text{total}} &= V_{\text{SUSY}} + V_{\text{Soft}} \\ &= \kappa^2 \left| M_*^2 - \frac{(H^c)^4}{m_P^2} + \frac{\lambda}{\kappa} h^2 \right|^2 + \frac{8\kappa^2 |S|^2 |H^c|^6}{m_P^4} + 4\lambda^2 h^2 |S|^2 \\ &\quad + \frac{a m_{3/2} \kappa M^4 |S|}{m_P^2} + M_S^2 |S|^2. \end{aligned} \quad (3.16)$$

During inflation, the soft mass terms are suppressed, but they can induce a small shift in the VEV of S from zero. Substituting the SUSY VEVs of H^c , \bar{H}^c , and h from Eq. (3.3) into V_{total} and aligning S along the real axis via an appropriate R -transformation, the total potential simplifies to:

$$V_{\text{total}}(S) = \frac{8\kappa^2 S^2 M^6}{m_P^4} + \frac{a m_{3/2} \kappa M^4 S}{m_P^2}, \quad (3.17)$$

where $a = 1$ and $M_S \ll M$ are assumed. Minimizing V_{total} with respect to S yields a non-zero VEV for S :

$$\frac{d}{dS} V_{\text{Total}}(S) = 0 \quad \Rightarrow \quad \langle S \rangle \simeq -\frac{m_{3/2}}{16\kappa} \left(\frac{m_P}{M} \right)^2. \quad (3.18)$$

The μ term is then generated from the $\lambda S h^2$ term in Eq. (2.4):

$$\mu \simeq \lambda \langle S \rangle = -\frac{\lambda m_{3/2}}{16\kappa} \left(\frac{m_P}{M} \right)^2 = -\frac{\lambda m_{3/2}}{16\kappa} \left(\frac{M}{M_*} \right)^2. \quad (3.19)$$

The stability of the inflationary trajectory with respect to fluctuations in the h_u and h_d fields can be evaluated by computing their mass spectrum during inflation. The mass-squared of these fields during inflation is given by

$$m_{h_{\pm}}^2 = S^2 \lambda^2 \pm \kappa \lambda \left(M_*^2 - \frac{M^8}{36 m_P^2 S^4} \right) \simeq S^2 \lambda^2 \pm \kappa \lambda M_*^2, \quad (3.20)$$

where the term $\kappa \lambda (M^4/6m_P S^2)^2$ is highly suppressed and can be ignored. The mass-squared $m_{h_-}^2 > 0$ requires,

$$\lambda > \frac{\kappa M_*^2}{S^2}. \quad (3.21)$$

In the smooth μ -hybrid inflation model, the H^c - \bar{H}^c system does not have a critical point, unlike the standard and shifted μ -hybrid inflation scenarios, which feature two critical points and a hierarchy between κ and λ to ensure H^c - \bar{H}^c stabilizes before h_u - h_d . Instead, the smooth model has a single critical point in the h_u - h_d system, with λ constrained to satisfy $S_{\text{end}} > S_c$.

3.2 Reheating and Non-Thermal Leptogenesis

After the end of inflation, the inflaton system, composed of two complex scalar fields: S and $\theta = (\delta\phi + \delta\bar{\phi})/\sqrt{2}$ (where $\delta\phi = \langle H^c \rangle - M$ and $\delta\bar{\phi} = \langle \bar{H}^c \rangle - M$) with mass m_I , descends toward the SUSY minimum, experiences damped oscillations about it, and eventually undergoes decay, initiating the process referred to as 'reheating'. We consider the non-thermal leptogenesis scenario [46–48] to account for the observed

baryon asymmetry. The superpotential term $\lambda S h^2$ induces an inflaton decay into a pair of higgsinos (\tilde{h}_u, \tilde{h}_d) and higgses (h_u, h_d), each with a decay width, Γ_h , given by [49],

$$\Gamma_h = \Gamma(\theta \rightarrow \tilde{h}_u \tilde{h}_d) = \Gamma(S \rightarrow h_u h_d) = \frac{\lambda^2}{8\pi} m_I, \quad (3.22)$$

where the inflaton mass m_I is given by

$$m_I = 2\sqrt{2} \kappa \left(\frac{M_*^2}{M} \right) = 2\sqrt{2} \kappa \left(\frac{M^3}{m_P^2} \right). \quad (3.23)$$

The right-handed neutrino mass receives contribution from the following superpotential term,

$$W \supset \alpha_1^{ij} F_i^c F_j^c \frac{\tilde{H}^c \tilde{H}^c}{m_P} \supset M_{\nu_i} \nu_i^c \nu_j^c, \quad (3.24)$$

with a Majorana mass matrix $\alpha_{ij}(M^2/m_P)$ and eigenvalues

$$M_{\nu_i} = \alpha_i \frac{M^2}{m_P}. \quad (3.25)$$

We assume hierarchical RHN Majorana masses with $M_{\nu_1} \ll M_{\nu_2}, M_{\nu_3}$ and $M_{\nu_1} > T_{\text{RH}}$. The inflaton decays into a pair of right-handed neutrinos (ν_i^c) and sneutrinos ($\tilde{\nu}_i^c$) with an equal decay width given as,

$$\begin{aligned} \Gamma_{\nu_i} &= \Gamma(\theta \rightarrow \nu_i^c \nu_i^c) = \Gamma(S \rightarrow \tilde{\nu}_i^c \tilde{\nu}_i^c) \\ &= \frac{m_I}{8\pi} \left(\frac{M_{\nu_i}}{M} \right)^2 \left(1 - \frac{4M_{\nu_i}^2}{m_I^2} \right)^{1/2}, \end{aligned} \quad (3.26)$$

provided that only the lightest right-handed neutrino with mass M_{ν_1} satisfies the kinematic bound, $m_I > 2M_{\nu_1}$.

With $H = 3\Gamma_I$, the reheat temperature T_{RH} is expressed in terms of the total decay width of the inflaton, Γ_I , as

$$T_{\text{RH}} = \left(\frac{90}{\pi^2 g_*} \right)^{1/4} \sqrt{\Gamma_I m_P}, \quad (3.27)$$

where $\Gamma_I = \Gamma_h + \Gamma_{\nu_1}$, and g_* is the effective number of relativistic degrees of freedom at the temperature T_{RH} , which, for the MSSM spectrum, is $g_* = 228.75$. Assuming a standard thermal history, the number of e-folds, N_0 , can be written in terms of the reheat

temperature, T_{RH} , as [50],

$$N_0 = 53 + \frac{1}{3} \ln \left[\frac{T_{\text{RH}}}{10^9 \text{ GeV}} \right] + \frac{2}{3} \ln \left[\frac{\sqrt{\kappa} M_*}{10^{15} \text{ GeV}} \right]. \quad (3.28)$$

While Γ_h is the dominant decay channel ($\Gamma_I \simeq \Gamma_h$), the Γ_{ν_1} channel is important for successful leptogenesis, which, through the sphaleron process [51–53], partially converts into the observed baryon asymmetry of the Universe (BAU). With $M_{\nu_1} \gg T_{\text{RH}}$, the washout factor of lepton asymmetry can be suppressed. The observed baryon asymmetry is evaluated in terms of the lepton asymmetry factor, ε_L [24],

$$\frac{n_B}{n_\gamma} \simeq -1.84 \varepsilon_L \frac{\Gamma_{\nu_1}}{\Gamma_I} \frac{T_{\text{RH}}}{m_I} \delta_{\text{eff}}, \quad (3.29)$$

where $|\delta_{\text{eff}}| \leq 1$ is the CP violating phase factor and the observed baryon-to-photon ratio, $n_B/n_\gamma = (6.12 \pm 0.04) \times 10^{-10}$ [54]. For hierarchical neutrino masses, the lepton-number asymmetry ε_L is given by [24, 55, 56],

$$\varepsilon_L \simeq -\frac{3}{8\pi} \frac{\sqrt{\Delta m_{31}^2} M_{\nu_1}}{\langle h_u \rangle^2}. \quad (3.30)$$

Here, the atmospheric neutrino mass squared difference is $\Delta m_{31}^2 \approx 2.6 \times 10^{-3} \text{ eV}^2$ and $\langle h_u \rangle \simeq 174 \text{ GeV}$ in the large $\tan \beta$ limit. For $|\delta_{\text{eff}}| = 1$ and using $\Gamma_h/\Gamma_{\nu_1} \simeq \lambda^2 (M/M_{\nu_1})^2$, we obtain the right-handed neutrino mass in terms of the reheat temperature

$$M_{\nu_1} \simeq \left(\frac{n_B}{n_\gamma} \left(\frac{8\pi}{5.52} \right) \frac{\lambda^2 \langle h_u \rangle^2 m_I M^2}{\sqrt{\Delta m_{31}^2} T_{\text{RH}}} \right)^{1/3}. \quad (3.31)$$

For successful leptogenesis, the above equation must satisfy the kinematic bound $m_I \geq 2M_{\nu_1}$.

3.3 Inflationary Observables

The prediction of various inflationary parameters can now be estimated using standard slow-roll definitions described below. The leading order slow-roll parameters are defined as

$$\begin{aligned} \epsilon(z) &= \frac{1}{4} \left(\frac{m_P}{M} \right)^2 \left(\frac{V'(z)}{V(z)} \right)^2, \quad \eta(z) = \frac{1}{2} \left(\frac{m_P}{M} \right)^2 \left(\frac{V''(z)}{V(z)} \right), \\ \xi^2(z) &= \frac{1}{4} \left(\frac{m_P}{M} \right)^4 \left(\frac{V'(z)V'''(z)}{V^2(z)} \right), \end{aligned} \quad (3.32)$$

where the derivatives are with respect to $z = |S|/M$. In the slow-roll (leading order) approximation, the tensor-to-scalar ratio r , the scalar spectral index n_s , and the running of the scalar spectral index $dn_s/d \ln k$ are given by

$$r \simeq 16 \epsilon(z), \quad (3.33)$$

$$n_s \simeq 1 + 2 \eta(z) - 6 \epsilon(z), \quad (3.34)$$

$$\frac{dn_s}{d \ln k} \simeq 16 \epsilon(z) \eta(z) - 24 \epsilon^2(z) - 2 \xi^2(z). \quad (3.35)$$

The amplitude of the curvature perturbation is given by

$$A_s(k_0) = \frac{1}{24 \pi^2} \left(\frac{V/m_P^4}{\epsilon} \right) \Big|_{z=z_0}. \quad (3.36)$$

where $A_s = 2.1 \times 10^{-9}$ is the Planck normalization at $k_0 = 0.05 \text{ Mpc}^{-1}$ [1]. The last N_0 number of e -folds before the end of inflation is,

$$N_0 = 2 \left(\frac{M}{m_P} \right)^2 \int_{z_e}^{z_0} \left(\frac{V}{V'} \right) dz, \quad (3.37)$$

where z_0 is the field value at the pivot scale k_0 , and z_e is the field value at the end of inflation, defined by $|\eta(z_e)| = 1$.

3.4 Inflationary Predictions and Comparison with Observations

The constraints on the scalar spectral index n_s and the tensor-to-scalar ratio r in the $\Lambda\text{CDM} + r$ model from the Planck 2018 CMB power spectra, in combination with CMB lensing reconstruction and BICEP2/Keck Array (BK15) data at the 95 % confidence level, are [1]:

$$\left. \begin{array}{l} n_s = 0.9651 \pm 0.0041, \\ r < 0.061, \end{array} \right\} \begin{array}{l} 95 \%, \text{ Planck TT,TE,EE} \\ \text{+lowE+lensing+BK15.} \end{array} \quad (3.38)$$

It can be easily verified that, in the case of the minimal Kähler potential (with $\kappa_S = \kappa_{SS} = 0$), SUGRA corrections dominate the global SUSY potential. This leads to the prediction of n_s and r inconsistent with the above bounds. In simpler terms, the SUGRA corrections necessitate trans-Planckian field values to achieve n_s and r within experimental bounds, thereby invalidating the SUGRA expansion itself. Consequently, the minimal case ($\kappa_S = \kappa_{SS} = 0$) is inconsistent with the current observations.

The results of our numerical calculations for the inflationary potential in Eq. (3.15) with a non-minimal Kähler potential are displayed in Figs. 2 - 6. To obtain these results, a second-order approximation has been employed for the slow-roll parameters, and the scalar spectral index n_s has been fixed at the central value (~ 0.9651) of Planck's 2018

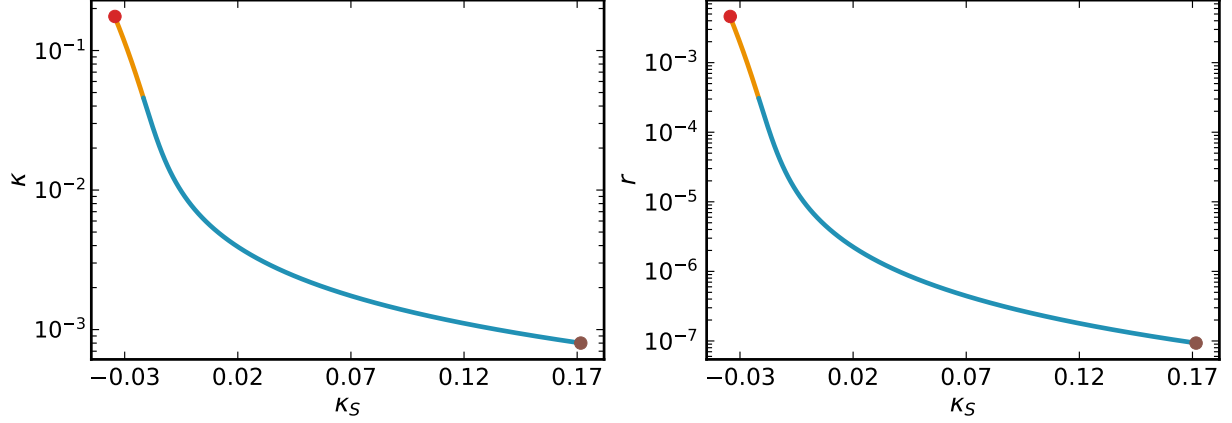


Figure 2: Variation of dimensionless parameter κ (left) and tensor-to-scalar ratio r (right) with the non-minimal coupling κ_S . The yellow and blue curves represent field values $|S_0| \gtrsim 0.5 m_P$ and $|S_0| \lesssim 0.5 m_P$, respectively. The red and brown circles correspond to $|S_0| = m_P$ and $\kappa_{SS} = -1$ constraints, respectively.

data bounds. Additionally, the soft SUSY masses have been set at $m_{3/2} \simeq M_S \simeq 100$ TeV, with $a = 1$. Note that for $m_{3/2} \simeq 100$ TeV, there is no upper bound on the reheat temperature T_{RH} [57, 58]. We further set the mass parameter $M_* \simeq 2 \times 10^{16}$ GeV, which in turn determines $M = \sqrt{M_* m_P} \simeq 2.2 \times 10^{17}$ GeV. The right-hand side of the inequality (3.21) varies between $\simeq 1.2 \times 10^{-5} - 1.5 \times 10^{-6}$ for the range of parameters obtained in our numerical calculations. Therefore, we set $\lambda \sim 2 \times 10^{-5}$ in our analysis. This choice ensures that both the kinematic bound ($m_I \geq 2M_{\nu_1}$) and the out-of-equilibrium condition for leptogenesis ($M_{\nu_1} > T_{RH}$) are easily met.

The SUGRA corrections, parameterized by κ_S and κ_{SS} , dominate the global SUSY potential, while the soft mass terms with $m_{3/2} \simeq M_S \simeq 100$ TeV are highly suppressed. To keep the SUGRA expansion under control, we impose $|S_0| \leq m_P$. Additionally, we restrict the non-minimal couplings $|\kappa_S| \leq 1$ and $|\kappa_{SS}| \leq 1$. These constraints are depicted in Figs. 2 - 6 by the red ($|S_0| = m_P$) and brown ($\kappa_{SS} = -1$) circles. The yellow region, with $|S_0| \gtrsim 0.5 m_P$, represents the ultraviolet sensitivity region where higher-order Planck-suppressed terms in the SUGRA expansion become important. On the other hand, the blue region represents $|S_0| \lesssim 0.5 m_P$, where a natural suppression of higher-order terms is achieved along with the boundedness of the potential. This issue arises due to the quartic coupling being $\gamma_S < 0$. It is evident that both the quadratic (κ_S) and quartic (γ_S) couplings play a vital role in bringing the scalar spectral index n_s within the Planck bounds, accompanied by a large value of the tensor-to-scalar ratio r .

The behavior of the tensor-to-scalar ratio r and the dimensionless parameter κ , as displayed in Fig. 2, can be understood through the following explicit relationship

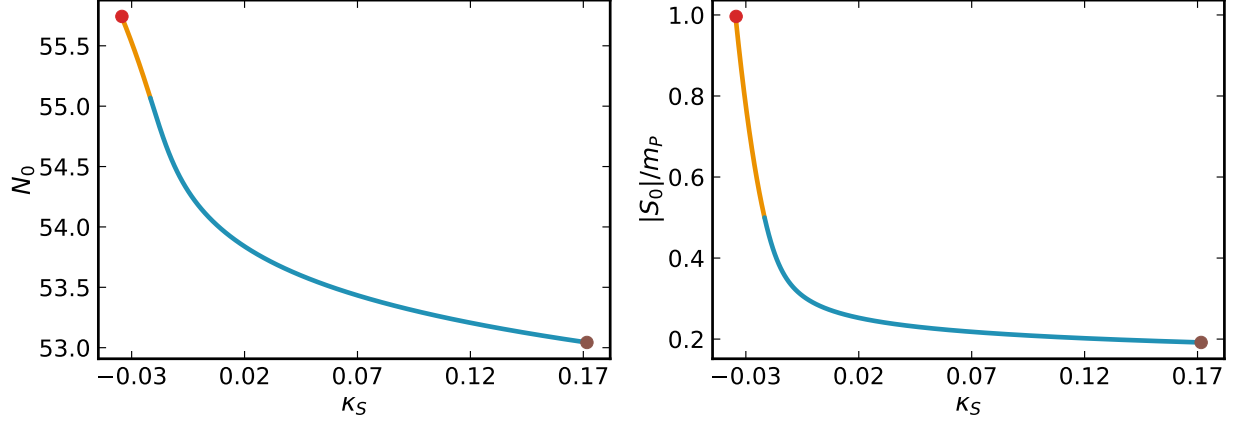


Figure 3: Variation of number of e -folds N_0 (left) and $|S_0|/m_P$ (right) with the non-minimal coupling κ_S . The yellow and blue curves represent field values $|S_0| \gtrsim 0.5 m_P$ and $|S_0| \lesssim 0.5 m_P$, respectively. The red and brown circles correspond to $|S_0| = m_P$ and $\kappa_{SS} = -1$ constraints, respectively.

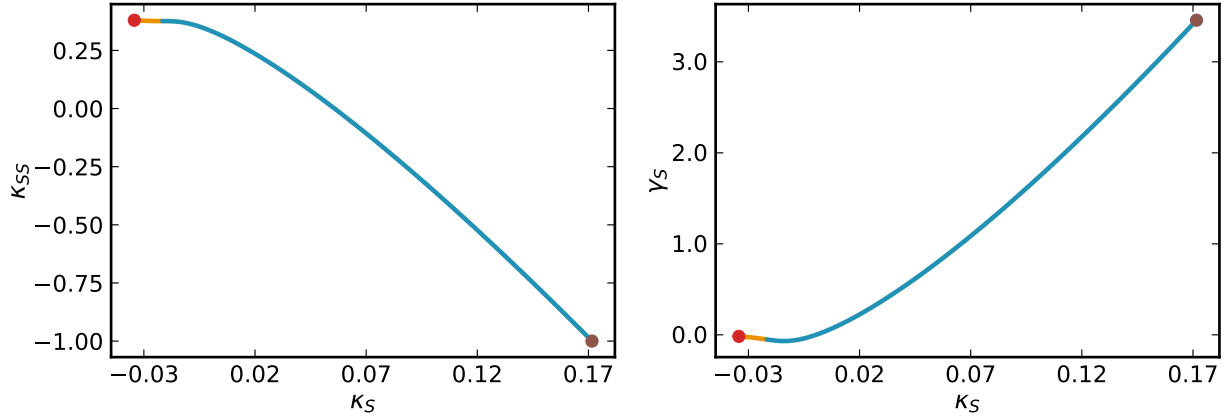


Figure 4: Variation of non-minimal coupling κ_{SS} (left) and quartic coupling γ_S (right) with the non-minimal coupling κ_S . The yellow and blue curves represent field values $|S_0| \gtrsim 0.5 m_P$ and $|S_0| \lesssim 0.5 m_P$, respectively. The red and brown circles correspond to $|S_0| = m_P$ and $\kappa_{SS} = -1$ constraints, respectively.

between r , κ and M

$$r \simeq \left(\frac{2\kappa^2}{3\pi^2 A_s(k_0)} \right) \left(\frac{M}{m_P} \right)^8 \simeq \kappa^2 \left(\frac{M}{3.23 \times 10^{16} \text{ GeV}} \right)^4 \left(\frac{M}{m_P} \right)^4. \quad (3.39)$$

Since M is fixed, larger values of r are expected for large values of κ . It can readily be checked that the largest value of r ($\sim 4 \times 10^{-3}$) obtained in our numerical results occurs for $\kappa \simeq 0.17$. The behavior of the last number of e -folds N_0 and $|S_0|/m_P$ with respect to κ_S is presented in Fig. 3, while Fig. 4 depicts the behavior of κ_{SS} and γ_S with respect to

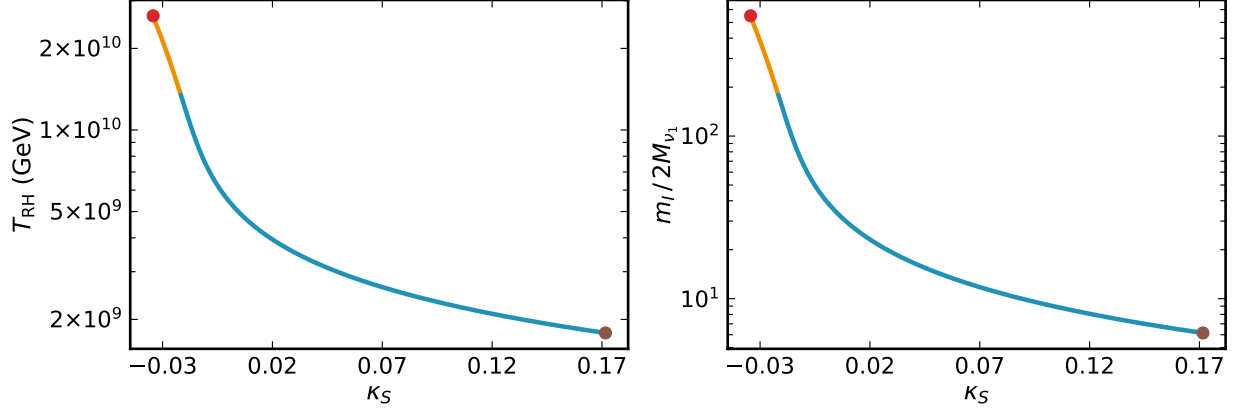


Figure 5: Variation of the reheat temperature T_{RH} (left) and the inflaton mass to RHN mass ratio $m_I/2M_{\nu_1}$ (right) with the non-minimal coupling κ_S . The yellow and blue curves represent field values $|S_0| \gtrsim 0.5 m_P$ and $|S_0| \lesssim 0.5 m_P$, respectively. The red and brown circles correspond to $|S_0| = m_P$ and $\kappa_{SS} = -1$ constraints, respectively.

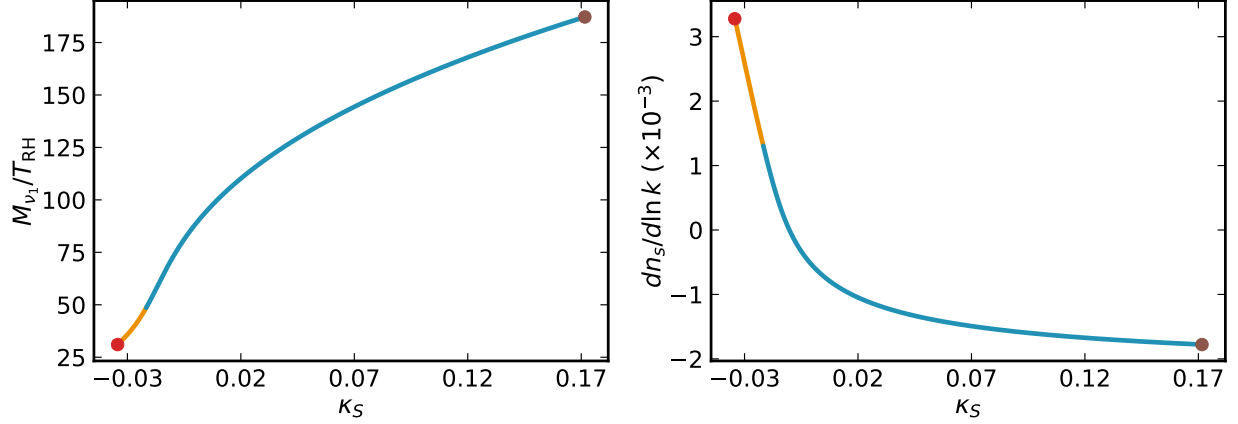


Figure 6: Variation of the ratio M_{ν_1}/T_{RH} (left) and the running of the scalar spectral index $dn_s/d \ln k$ (right) with the non-minimal coupling κ_S . The yellow and blue curves represent field values $|S_0| \gtrsim 0.5 m_P$ and $|S_0| \lesssim 0.5 m_P$, respectively. The red and brown circles correspond to $|S_0| = m_P$ and $\kappa_{SS} = -1$ constraints, respectively.

κ_S . The number of e -folds vary within the range $53 \lesssim N_0 \lesssim 56$. It can be seen that the large r values are obtained with non-minimal couplings $\kappa_S < 0$, $\kappa_{SS} > 0$ and the quartic coupling $\gamma_S < 0$. Also, the large r values occur for tiny values of the quartic coupling γ_S (~ -0.02). To facilitate this discussion further, we provide an analytical estimate of the couplings κ_S and γ_S in the large r region, where the contribution from the global SUSY part of the potential is negligible, and $|S_0|$ approaches m_P . Using Eqs. (3.33), (3.34) and (3.37) with $|S_0| \simeq m_P$, we obtain the following approximate expressions for number of

e -folds N_0 , scalar spectral index n_s and tensor to scalar ratio r

$$N_0 \simeq \frac{1}{6\kappa_S} \log \left(- \left(\frac{2 \times 10^{17} \text{ GeV}}{m_P} \right)^2 \frac{(\gamma_S - \kappa_S)^4}{\kappa_S^3} \right), \quad (3.40)$$

$$n_s \simeq 1 + \frac{10}{27z_0^6} \left(\frac{m_P}{M} \right)^2 - 2\kappa_S + 6\gamma_S z_0^2 \left(\frac{M}{m_P} \right)^2 \simeq 1 - 2\kappa_S + 6\gamma_S, \quad (3.41)$$

$$r \simeq 16 \left(\frac{1}{27z_0^5} \left(\frac{m_P}{M} \right)^3 - \kappa_S z_0 \left(\frac{M}{m_P} \right) + \gamma_S z_0^3 \left(\frac{M}{m_P} \right)^3 \right)^2 \simeq 16 (\gamma_S - \kappa_S)^2. \quad (3.42)$$

Solving Eqs. (3.40) and (3.41) simultaneously for $N_0 \simeq 55$ and $n_s \simeq 0.9651$, we obtain $\kappa_S \sim -0.034$ and $\gamma_S \sim -0.017$. Using these values in Eq. (3.42), we obtain $r \sim 0.004$ which is a reasonably good estimate of the otherwise more accurately calculated numerical results displayed in Figs. 2 - 6. Note that the large tensor modes require values of M greater than the GUT scale $M_{\text{GUT}} \simeq 2 \times 10^{16}$ GeV. Figure 5 illustrates the variation of the reheat temperature, T_{RH} , and the ratio of the inflaton mass to the right-handed neutrino (RHN) mass, $m_I/2M_{\nu_1}$. Meanwhile, Figure 6 shows the variation of the ratio M_{ν_1}/T_{RH} and the running of the scalar spectral index, $dn_s/d \ln k$, with respect to κ_S . The reheat temperature varies in the range $1.8 \times 10^9 \text{ GeV} \lesssim T_{\text{RH}} \lesssim 2.6 \times 10^{10} \text{ GeV}$, with the kinematic bound $m_I \geq 2M_{\nu_1}$ satisfied across the entire range of κ_S . Additionally, since $T_{\text{RH}} < M_{\nu_1}$, the out-of-equilibrium condition for successful leptogenesis is easily met. The running of the scalar spectral index ranges from $-0.0018 \lesssim dn_s/d \ln k \lesssim 0.0033$, consistent with the $\Lambda\text{CDM}+r$ model assumptions. The MSSM μ -term of $\mathcal{O}(1)$ TeV can be generated from Eq. (3.19) with $\lambda \sim 2 \times 10^{-5}$, $\kappa \sim 0.015$, and a gravitino mass $m_{3/2} \simeq 100$ TeV.

In summary, for non-minimal couplings $-0.034 \lesssim \kappa_S \lesssim 0.17$ and $-1 \lesssim \kappa_{SS} \lesssim 0.38$, with the scalar spectral index fixed at the central value ($n_s \simeq 0.9651$) of Planck 2018 data bounds and M_* fixed at 2×10^{16} GeV, we obtain a tensor-to-scalar ratio $9.3 \times 10^{-8} \lesssim r \lesssim 4.6 \times 10^{-3}$. The inflaton mass ranges from 4.1×10^{12} GeV to 9.0×10^{14} GeV, and the RHN mass ranges from 3.3×10^{11} GeV to 8.2×10^{11} GeV, with α_1 in the range $1.7 \times 10^{-5} \lesssim \alpha_1 \lesssim 4.1 \times 10^{-5}$. The predictions of the model are thus perfectly compatible with current observations.

4 Non-Minimal Higgs Inflation

We utilize the same superpotential W as given in Eq. (2.4). In non-minimal Higgs inflation, the conjugate Higgs fields (H^c, \bar{H}^c) assume the role of the inflaton. To implement non-minimal Higgs inflation in the context of $G_{422} \equiv SU(4)_C \times SU(2)_L \times SU(2)_R$ model with a global $U(1)_R$ and a Z_2 symmetry, we adopt the following form of the Kähler

potential¹ [38]

$$K = -3m_P^2 \log \left(1 - \frac{(|S|^2 + |H^c|^2 + |\bar{H}^c|^2)}{3m_P^2} + \frac{\delta}{2m_P^4} \left((H^c \bar{H}^c)^2 + h.c. \right) \right. \\ \left. + \frac{\gamma}{3m_P^4} \left(|S|^4 + |S|^2 |H^c|^2 + |S|^2 |\bar{H}^c|^2 + |H^c|^4 + |\bar{H}^c|^4 \right) \right), \quad (4.1)$$

where δ and γ are dimensionless couplings that vanish in the exact no-scale limit and we have assumed the stabilization of the modulus fields [61–63]. The term with coupling δ plays a pivotal role in non-minimal Higgs inflation, while the higher-order term with the coupling γ is required to stabilize S during inflation [64]. It is worth noting that S can also be stabilized without the inclusion of quartic terms, as shown in [65, 66].

The scalar potential in the Einstein' frame is given by,

$$V_E = e^{G/m_P^2} \left(G_i (G^{-1})^i_j G^j - 3m_P^4 \right) + \frac{1}{2} g_a^2 G^i (T_a)_i^j z_j (\text{Re} f_{ab}^{-1}) G^k (T_b)_k^l z_l, \quad (4.2)$$

with

$$G = K + m_P^2 \log \left(\frac{|W|^2}{m_P^6} \right), \quad G^i = m_P \frac{\partial G}{\partial z_i}, \quad G_i = m_P \frac{\partial G}{\partial z_i^*}, \quad G_j^i = \frac{\partial G}{\partial z_i \partial z_j^*}, \quad (4.3)$$

where $z_i \in \{S, H^c, \bar{H}^c\}$, f_{ab} represents the gauge kinetic function, and T_a denotes the generators of the gauge group. Here, we have used the same notation for both the superfields and their corresponding scalar components. The complex Higgs fields can be expressed in terms of real scalar fields as follows:

$$H^c = \frac{w}{\sqrt{2}} e^{i\theta} \cos \phi, \quad \bar{H}^c = \frac{w}{\sqrt{2}} e^{i\bar{\theta}} \sin \phi. \quad (4.4)$$

In the D -flat direction, the phases can be stabilized at $\theta = \bar{\theta} = 0$, $\phi = \pi/4$, leading to:

$$H^c = \bar{H}^c = \frac{w}{2}, \quad (4.5)$$

where w represents the real scalar field in the Jordan frame. The scalar potential in the

¹It has recently been shown in [59] that incorporating a sextic term ($|S|^6/m_P^6$) in the Kähler potential plays a crucial role in the generation of primordial black holes (PBH). In another study [60], a cubic term of the form S^3/m_P^3 is shown to play a similar role in generating PBHs, where $U(1)_R$ symmetry is assumed to be broken at the non-renormalizable level.

Einstein frame then takes the form:

$$V_E = \frac{\kappa^2 M_*^4 \left(1 - \left(\frac{w}{2M}\right)^4\right)^2}{\left(1 - 2\gamma \left(\frac{w}{2m_P}\right)^2\right) \left(1 - \frac{2}{3} \left(\frac{w}{2m_P}\right)^2 + \frac{1}{3} (3\delta + 2\gamma) \left(\frac{w}{2m_P}\right)^4\right)^2}$$

$$= \frac{\kappa^2 M_*^4}{\Omega^2} \left(1 - \left(\frac{w}{2M}\right)^4\right)^2 \left(1 - 2\gamma \left(\frac{w}{2m_P}\right)^2\right)^{-1}, \quad (4.6)$$

where, $M = \sqrt{M_* m_P}$ and the conformal scaling factor, $\Omega = e^{-K/3m_P^2}$, which relates the Einstein and Jordan frames, is given by

$$g_{\mu\nu}^J = \Omega g_{\mu\nu}^E = \left(1 - \frac{2}{3} \left(\frac{w}{2m_P}\right)^2 + \frac{1}{3} (3\delta + 2\gamma) \left(\frac{w}{2m_P}\right)^4\right) g_{\mu\nu}^E. \quad (4.7)$$

The action in the Einstein' frame is

$$S_E = \int d^4x \sqrt{-g_E} \left[\frac{1}{2} m_P^2 \mathcal{R}(g_E) - \frac{1}{2} g_E^{\mu\nu} \partial_\mu \widehat{w} \partial_\nu \widehat{w} - V_E(\widehat{w}(w)) \right], \quad (4.8)$$

where \widehat{w} is the canonically normalized inflaton field in the Einstein frame, defined as

$$\frac{d\widehat{w}}{dw} \equiv J(w) = \sqrt{\frac{1}{\Omega(w)} + \frac{3}{2} m_P^2 \left(\frac{\Omega'(w)}{\Omega(w)}\right)^2}. \quad (4.9)$$

4.1 MSSM μ -Term

Following [67], we derive the MSSM μ term within the framework of the non-minimal Higgs inflation model. The scalar potential in the SUSY limit is expressed as [68]:

$$V_{\text{SUSY}} = \widetilde{K}^{\alpha\bar{\beta}} W_\alpha W_{\bar{\beta}}^* + \frac{g^2}{2} \sum_a D_a D_a, \quad (4.10)$$

where the superpotential W is provided in Eq. (2.4), and \widetilde{K} represents the $m_P \rightarrow \infty$ limit of the Kähler potential in Eq. (4.1), given by:

$$\widetilde{K} = |S|^2 + |H^c|^2 + |\bar{H}^c|^2 - \frac{3\delta}{2m_P^2} \left((H^c \bar{H}^c)^2 + h.c \right)$$

$$- \frac{\gamma}{m_P^2} \left(|S|^4 + |S|^2 |H^c|^2 + |S|^2 |\bar{H}^c|^2 + |H^c|^4 + |\bar{H}^c|^4 \right) + \dots. \quad (4.11)$$

Using Eqs. (4.11) and (2.4) into Eq. (4.10), the SUSY potential in the D -flat direction, after substituting the VEVs from Eq. (3.3), becomes

$$V_{\text{SUSY}} = 8\kappa^2 S^2 M^2 \left(\frac{M}{m_P} \right)^4 \left(1 - 5\delta \left(\frac{M}{m_P} \right)^4 \right)^{-1}. \quad (4.12)$$

The soft SUSY breaking terms, while negligible during inflation, can cause a slight shift in the VEV of S from zero. Including the soft SUSY breaking terms from Eq. (3.9), the total SUSY potential can be written as

$$\begin{aligned} V_{\text{Total}}(S) &= V_{\text{SUSY}}(S) + V_{\text{Soft}}(S), \\ &= 8\kappa^2 S^2 M^2 \left(\frac{M}{m_P} \right)^4 \left(1 - 5\delta \left(\frac{M}{m_P} \right)^4 \right)^{-1} + \kappa m_{3/2} S M^2 \left(\frac{M}{m_P} \right)^2, \end{aligned} \quad (4.13)$$

where we have used the fact that $M_S \ll M$ and have set $a = 1$. Minimizing the total potential with respect to S yields the following non-zero VEV for S ,

$$\frac{d}{dS} V_{\text{Total}}(S) = 0 \quad \Rightarrow \quad \langle S \rangle \simeq \frac{m_{3/2}}{16\kappa} \left(5\delta \left(\frac{M}{m_P} \right)^2 - \left(\frac{m_P}{M} \right)^2 \right). \quad (4.14)$$

The μ term is then generated from the $\lambda S h^2$ term in Eq. (2.4):

$$\mu \simeq \lambda \langle S \rangle = \frac{\lambda m_{3/2}}{16\kappa} \left(5\delta \left(\frac{M}{m_P} \right)^2 - \left(\frac{m_P}{M} \right)^2 \right). \quad (4.15)$$

Note that in the limit $\delta \rightarrow 0$, the μ term above simplifies to the same expression derived in the smooth hybrid inflation model, as given in Eq. (3.19).

The stability of the inflationary trajectory with respect to fluctuations in the h_u and h_d fields can be evaluated by computing their mass spectrum during inflation. The mass-squared of these fields during inflation is found to be:

$$m_{h_{\pm}}^2 = 4H_I^2 \left(\frac{1}{\Omega(w)} \pm \frac{12m_P^4 \lambda}{\kappa w^4} \right), \quad (4.16)$$

where $H_I^2 \simeq \frac{V_E}{3m_P^2}$. The condition $m_{h_-}^2 > 0$ requires:

$$\lambda < \frac{\kappa w^4}{12 \Omega m_P^4} \simeq \frac{4\kappa}{3\delta}. \quad (4.17)$$

4.2 Reheating and Non-Thermal Leptogenesis

After the end of inflation, the inflaton continues to roll towards the SUSY vacuum, eventually settling into a phase of damped oscillations. Subsequently, the inflaton decays, initiating the reheating of the universe. The decay widths of the inflaton decay into a pair of higgsinos (\tilde{h}_u, \tilde{h}_d) and a pair of right-handed neutrinos (ν_i^c) [27] are respectively given by

$$\Gamma_h = \frac{\lambda^2}{8\pi\Omega_0^2} m_I, \quad (4.18)$$

$$\Gamma_{\nu_i} = \frac{m_I}{64\pi} \left(\frac{M_{\nu_i}}{M} \frac{\Omega_0^{3/2}}{J_0} \right)^2 \left(1 + \left(\frac{M}{m_P} \right)^2 - \frac{1}{2} (3\delta + 2\gamma) \left(\frac{M}{m_P} \right)^4 \right)^2 \left(1 - \frac{4M_{\nu_i}^2}{m_I^2} \right)^{1/2}, \quad (4.19)$$

where the inflaton mass m_I and the RHN mass M_{ν_i} are given as

$$m_I = \frac{4\kappa}{J_0\Omega_0} \left(\frac{M_*^2}{M} \right) = \frac{4\kappa}{J_0\Omega_0} \left(\frac{M^3}{m_P^2} \right), \quad M_{\nu_i} = \alpha_i \frac{M^2}{m_P \sqrt{\Omega_0}}, \quad (4.20)$$

with

$$\Omega_0 = \Omega(\langle w \rangle = 2M) = 1 - \frac{2}{3} \left(\frac{M}{m_P} \right)^2 + \frac{1}{3} (3\delta + 2\gamma) \left(\frac{M}{m_P} \right)^4, \quad (4.21)$$

$$J_0 = J(\langle w \rangle = 2M). \quad (4.22)$$

In the supergravity framework, the inflaton can spontaneously decay into MSSM particles [69, 70]. In the current SUSY GUT model, the Yukawa interaction for the third generation, $y_{33}^{(u,v)} Q_3 L_3 H_u$, gives rise to the following 3-body decay width [27],

$$\Gamma_{y_t} = \frac{7}{256\pi^3} \left(\frac{y_t \Omega_0^{3/2}}{J_0} \right)^2 \left(1 - (3\delta + 2\gamma) \left(\frac{M}{m_P} \right)^2 \right)^2 \left(\frac{M}{m_P} \right)^2 \left(\frac{m_I}{m_P} \right)^2 m_I, \quad (4.23)$$

where, $y_t = y_{33}^{(u,v)}$ corresponds to the top Yukawa coupling. The reheating temperature T_{RH} is expressed in terms of the inflaton decay width in Eq. (3.27), where the total decay width of the inflaton is now $\Gamma_I = \Gamma_{\nu_i} + \Gamma_h + \Gamma_{y_t}$. Using Eqs. (3.29), (3.30), (4.19), and assuming hierarchical RHN Majorana masses with $M_{\nu_1} \ll M_{\nu_2}, M_{\nu_3}$ and $M_{\nu_1} > T_{\text{RH}}$, we

obtain the right-handed neutrino mass in terms of the reheat temperature

$$M_{\nu_1} \simeq \left(\frac{n_B}{n_\gamma} \left(\frac{512\pi^2}{5.52} \right) \frac{(\Gamma_h + \Gamma_{y_t}) \langle h_u \rangle^2}{\sqrt{\Delta m_{31}^2} T_{\text{RH}}} \left(\frac{J_0 M}{\Omega_0^{3/2}} \right)^2 \left(1 + \left(\frac{M}{m_P} \right)^2 - \frac{1}{2} (3\delta + 2\gamma) \left(\frac{M}{m_P} \right)^4 \right)^{-2} \right)^{1/3}, \quad (4.24)$$

where $\Gamma_I \simeq \Gamma_h + \Gamma_{y_t}$, as the right-handed neutrino (RHN) channel is sub-dominant. For successful leptogenesis, the inflaton decay to right-handed neutrinos must be kinematically allowed, i.e., the above equation must satisfy the constraint $m_I \geq 2M_{\nu_1}$.

4.3 Inflationary Observables

The slow-roll parameters in Eq. (3.32) are modified and can now be expressed in terms of w as

$$\epsilon(w) = \frac{1}{2} m_P^2 \left(\frac{V'_E(w)}{J(w)V_E(w)} \right)^2, \quad (4.25)$$

$$\eta(w) = m_P^2 \left(\frac{V''_E(w)}{J^2(w)V_E(w)} - \frac{J'(w)V'_E(w)}{J^3(w)V_E(w)} \right), \quad (4.26)$$

$$\begin{aligned} \xi^2(w) = m_P^4 \left(\frac{V'_E(w)}{J^4(w)V_E(w)} \right) & \left(\frac{V'''_E(w)}{V_E(w)} - 3 \frac{J'(w)V''_E(w)}{J(w)V_E(w)} \right. \\ & \left. + 3 \frac{J'^2(w)V'_E(w)}{J^2(w)V_E(w)} - \frac{J''(w)V'_E(w)}{J(w)V_E(w)} \right), \end{aligned} \quad (4.27)$$

where a prime denotes a derivative with respect to w . The tensor-to-scalar ratio r , the scalar spectral index n_s , and the running of the scalar spectral index $dn_s/d \ln k$ to the first order in the slow-roll approximation are expressed as follows:

$$r \simeq 16\epsilon(w_0), \quad (4.28)$$

$$n_s \simeq 1 - 6\epsilon(w_0) + 2\eta(w_0), \quad (4.29)$$

$$\frac{dn_s}{d \ln k} \simeq 16 \epsilon(w_0) \eta(w_0) - 24 \epsilon^2(w_0) - 2 \xi^2(w_0). \quad (4.30)$$

The amplitude of the scalar power spectrum is given by

$$A_s(k_0) = \frac{1}{24\pi^2 m_P^4} \frac{V_E(w)}{\epsilon(w)} \bigg|_{w(k_0)=w_0}, \quad (4.31)$$

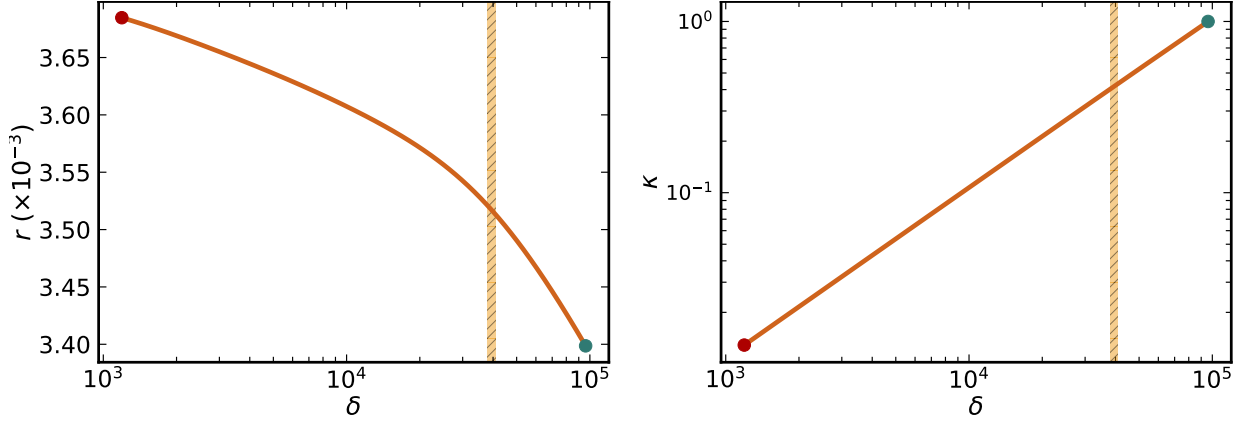


Figure 7: Variation of tensor-to-scalar ratio r (left) and dimensionless coupling κ (right) with the non-minimal coupling δ . The red and green circles correspond to $|w_0| = m_P$ and $\kappa = 1$ constraints, respectively. The small hatched region represents the parametric space where the kinematic condition ($m_I \geq 2M_{v_1}$) breaks down.

where w_0 is the field value at the pivot scale. The N_0 last number of e -folds from $w = w_0$ to the end of inflation at $w = w_e$ are expressed as:

$$N_0 = \frac{1}{m_P^2} \int_{w_e}^{w_0} \frac{J^2(w) V_E(w)}{V'_E(w)} dw, \quad (4.32)$$

where the number of e -folds N_0 are related to the reheat temperature T_{RH} as given in Eq. (3.28).

4.4 Inflationary Predictions and Comparison with Observations

The results of our analysis are depicted in Figs. 7 - 11, where various model parameters and inflationary observables are plotted against the non-minimal coupling δ . Throughout our analysis, we have set the scalar spectral index at the central observationally favored value of the Planck2018 + BICEP2/Keck Array (BK15) bounds ($n_s = 0.9651$) and fixed the mass parameter $M_* \simeq 10^{16}$ GeV, which determines $M = \sqrt{M_* m_P} \simeq 1.56 \times 10^{17}$ GeV. Additionally, we have ensured that the dimensionless parameter $\kappa \leq 1$ and that the field values remain sub-Planckian ($w_0 \leq m_P$). These constraints are indicated by the green and red circles, respectively. The right hand side of the inequality (4.17) yields $\simeq 1.4 \times 10^{-5}$. Therefore, we set $\lambda \simeq 1 \times 10^{-5}$ in our numerical calculations.

The hatched region in Figures 7 - 11 represents a small region of parametric space where the kinematic condition ($m_I \geq 2M_{v_1}$) breaks down, and as a result, it is excluded from our results. This can be understood from Eq. (4.24), where it can be seen that the

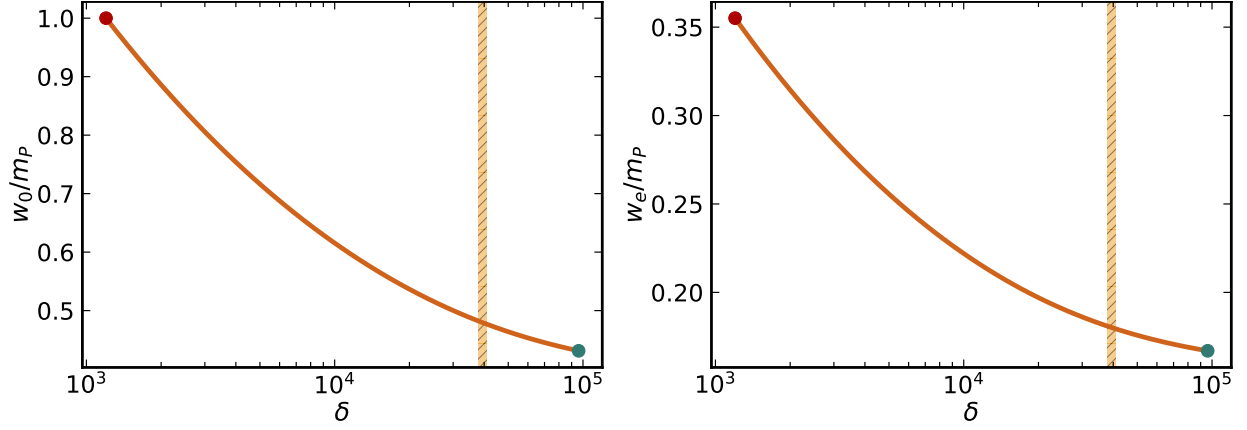


Figure 8: Variation of w_0/m_P (left) and w_e/m_P (right) with the non-minimal coupling δ . The red and green circles correspond to $|w_0| = m_P$ and $\kappa = 1$ constraints, respectively. The small hatched region represents the parametric space where the kinematic condition ($m_I \geq 2M_{\nu_1}$) breaks down.

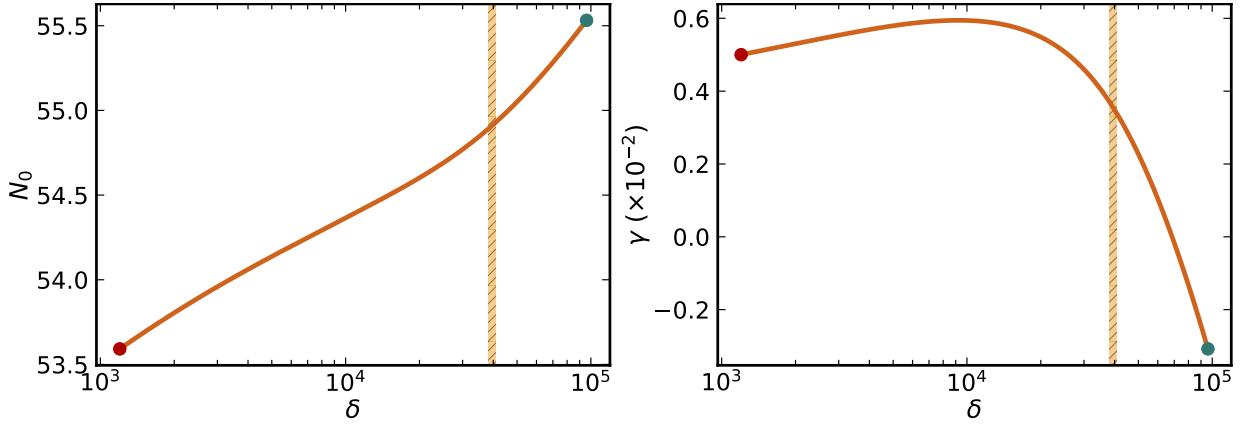


Figure 9: Variation of the last number of e -folds N_0 (left) and the non-minimal coupling γ (right) with the non-minimal coupling δ . The red and green circles correspond to $|w_0| = m_P$ and $\kappa = 1$ constraints, respectively. The small hatched region represents the parametric space where the kinematic condition ($m_I \geq 2M_{\nu_1}$) breaks down.

RHN mass M_{ν_1} depends on the following factor:

$$M_{\nu_1} \propto \left(1 + \left(\frac{M}{m_P} \right)^2 - \frac{1}{2} (3\delta + 2\gamma) \left(\frac{M}{m_P} \right)^4 \right)^{-2/3}, \quad (4.33)$$

which, for the coupling values $38111 \lesssim \delta \lesssim 40782$, approaches 0, leading to large M_{ν_1} . Consequently, M_{ν_1} becomes greater than the inflaton mass m_I , breaking the kinematic condition, as depicted in the left panel of Fig. 11. Outside this range of δ , the kinematic

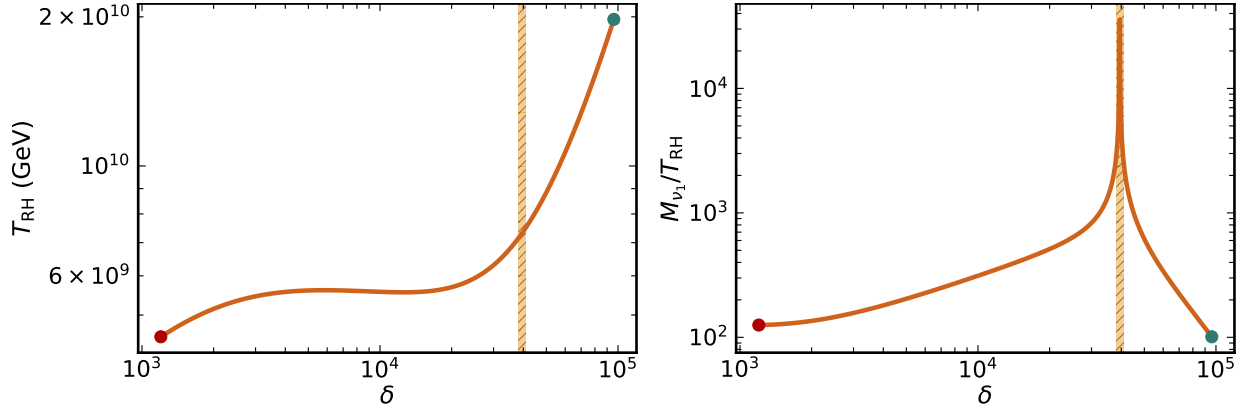


Figure 10: Variation of the reheat temperature T_{RH} (left) and the ratio M_{v_1}/T_{RH} (right) with the non-minimal coupling δ . The red and green circles correspond to $|w_0| = m_P$ and $\kappa = 1$ constraints, respectively. The small hatched region represents the parametric space where the kinematic condition ($m_I \geq 2M_{v_1}$) breaks down.

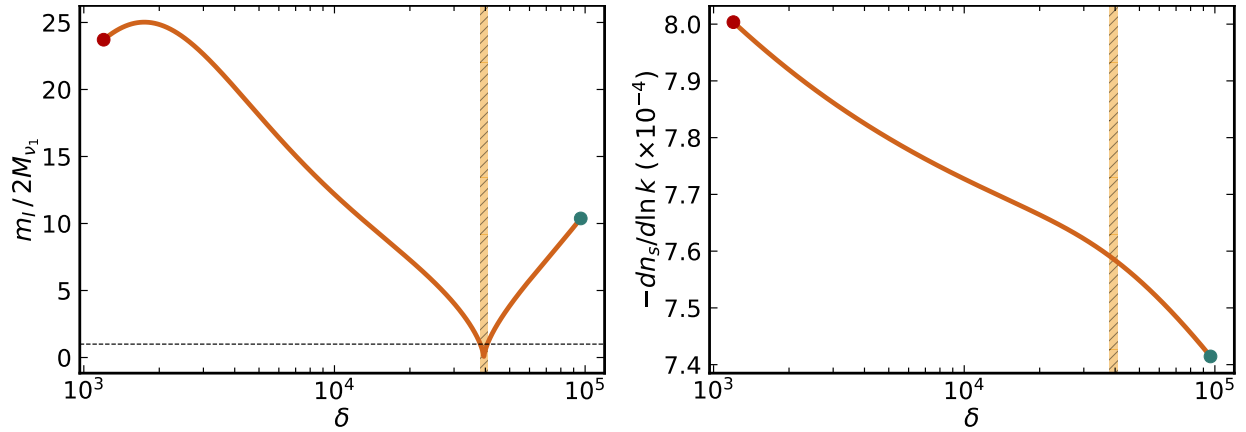


Figure 11: Variation of the ratio $m_I/2M_{v_1}$ (left) and the running of the scalar spectral index $dn_s/d \ln k$ (right) with the non-minimal coupling δ . The red and green circles correspond to $|w_0| = m_P$ and $\kappa = 1$ constraints, respectively. The small hatched region represents the parametric space where the kinematic condition ($m_I \geq 2M_{v_1}$) breaks down.

bound is easily satisfied. Note that the inflaton mass remains almost constant $m_I \simeq (2.7 - 4.2) \times 10^{13}$ GeV for the entire range of δ .

The variation of the tensor-to-scalar ratio r and the coupling κ is illustrated in Fig. 7, while Fig. 8 depicts the behavior of w_0 and w_e with respect to the non-minimal coupling δ . It can be seen that observable values of the tensor-to-scalar ratio are achieved in the range $3.37 \times 10^{-3} \lesssim r \lesssim 3.86 \times 10^{-3}$ across the entire range of δ . It is noteworthy that the field w_0 varies inversely with κ due to their inverse relationship: $w_0 \propto 1/\kappa^{1/4}$, as shown below. Fig. 9 shows the variation of the number of e -folds and the non-minimal coupling γ with δ . The number of e -folds varies slightly, ranging from $53.5 \lesssim N_0 \lesssim 55.5$,

while the coupling γ assumes very small values and does not affect the inflationary predictions. The variation of the reheat temperature is presented in Fig. 10, along with the ratio M_{ν_1}/T_{RH} , indicating that the out-of-equilibrium condition for leptogenesis is easily satisfied. Finally, Fig. 10 displays the running of the scalar spectral index, which ranges from $-0.0008 \lesssim dn_s/d \ln k \lesssim 0.00074$, consistent with the assumptions of the $\Lambda\text{CDM}+r$ model.

It is useful to provide analytical estimate of the values obtained in our numerical results. Using Eq. (4.26) with $\epsilon(w_e) = 1$ and Eq. (4.31) with Planck normalization constraint $A_s = 2.1 \times 10^{-9}$, we can express w_0 and w_e in terms of the non-minimal coupling δ and M as

$$\frac{w_0}{2m_P} \simeq \left(\frac{2^{5/2}\pi\sqrt{A_s}}{\kappa} \left(1 + \delta \left(\frac{M}{m_P} \right)^4 \right) \right)^{1/4}, \quad (4.34)$$

$$\frac{w_e}{2m_P} \simeq \left(\frac{2}{\sqrt{3}\delta} + \frac{13}{6} \left(\frac{M}{m_P} \right)^4 \right)^{1/4}. \quad (4.35)$$

Moreover, using Eqs. (4.32), (4.28), (4.29) and (4.30), we obtain the following approximate expressions for the number of e -folds N_0 , tensor-to-scalar ratio r , scalar spectral index n_s and the running of scalar spectral index $dn_s/d \ln k$:

$$N_0 \simeq \frac{3}{4} \left(\frac{\left(\frac{w_0}{2m_P} \right)^4 - \left(\frac{w_e}{2m_P} \right)^4}{\frac{1}{\delta} + \left(\frac{M}{m_P} \right)^4} \right), \quad (4.36)$$

$$r \simeq \frac{64}{3} \left(\frac{1}{\delta} + \left(\frac{M}{m_P} \right)^4 \right)^2 \left(\left(\frac{w_0}{2m_P} \right)^4 - \left(\frac{M}{m_P} \right)^4 \right)^{-2}, \quad (4.37)$$

$$n_s \simeq 1 - \frac{8}{3} \left(\frac{1}{\delta} + \left(\frac{M}{m_P} \right)^4 \right) \left(\left(\frac{w_0}{2m_P} \right)^4 + \left(\frac{M}{m_P} \right)^4 \right) \left(\left(\frac{w_0}{2m_P} \right)^4 - \left(\frac{M}{m_P} \right)^4 \right)^{-2}, \quad (4.38)$$

$$\frac{dn_s}{d \ln k} \simeq -\frac{14}{3} \left(\frac{2m_P}{w_0} \right)^8 \left(\frac{1}{\delta} + \left(\frac{M}{m_P} \right)^4 \right)^2. \quad (4.39)$$

Eliminating w_0 from Eqs. (4.34) and (4.36), we obtain an explicit relationship between κ and δ

$$\kappa \simeq \frac{3\sqrt{2}\pi A_s \delta}{N_0}, \quad (4.40)$$

which explains their behavior depicted in the right panel of Fig. 7. Next, we derive the expressions for ϕ_0 , n_s , r , and $dn_s/d \ln k$ as functions of the number of e -folds N_0 .

Neglecting w_e in Eq. (4.36), we express w_0 in terms of N_0 :

$$\frac{w_0}{2m_P} \simeq \left(\frac{4}{3} N_0 \left(\frac{1}{\delta} + \left(\frac{M}{m_P} \right)^4 \right) \right)^{1/4}. \quad (4.41)$$

Using this expression for w_0 in Eqs. (4.37) - (4.39) yields:

$$r \simeq \frac{12}{N_0^2}, \quad n_s \simeq 1 - \frac{2}{N_0}, \quad \frac{dn_s}{d \ln k} \simeq -\frac{21}{8N_0^2}. \quad (4.42)$$

It can be checked that for $N_0 \simeq 55$, these expressions yield $r \sim 0.004$, $n_s \sim 0.964$ and $dn_s/d \ln k \sim -0.0008$. These values closely align with the more precise results displayed in Figs. 7 - 11. The MSSM μ term of $\mathcal{O}(1)$ TeV, can be obtained from Eq. (4.15) with $m_{3/2} \simeq 100$ TeV, $\kappa \simeq 0.013$, $\delta \simeq 25000$ and $\lambda \simeq 10^{-5}$.

In summary, for non-minimal coupling $1200 \lesssim \delta \lesssim 96000$, we obtain $0.013 \lesssim \kappa \lesssim 1$, number of e -folds $53.5 \lesssim N_0 \lesssim 55.5$, and the RHN mass in the range $5.6 \times 10^{11} \text{ GeV} \lesssim M_{\nu_1} \lesssim 1.6 \times 10^{14} \text{ GeV}$ with the coupling $5.7 \times 10^{-5} \lesssim \alpha_1 \lesssim 2 \times 10^{-2}$. The scalar spectral index closely aligns with the central value of Planck's bounds along with observable values of the tensor-to-scalar ratio $r \sim 3 \times 10^{-3}$. The non-minimal coupling δ takes on large values² ($\sim 10^5$), a characteristic feature of non-minimal Higgs inflation models.

5 Observable Primordial Gravitational Waves

The distinctive signature of the tensor signal primarily manifests in the degree scales of the CMB B-mode polarization. Numerous experiments have already been conducted, and others are currently underway, aimed at measuring the B-mode power. The tensor-to-scalar ratio " r ," which parameterizes the amplitude of primordial gravitational waves, is poised to be measured with significant precision by numerous forthcoming experiments. These experiments encompass a range of missions, including the Simons Observatory [78], which aims to achieve a measurement of r with $\delta r = 0.003$. CMB-S4 (Cosmic Microwave Background Stage 4) [79, 80], on the other hand, seeks to detect $r \gtrsim 0.003$ at a significance level exceeding 5σ , or establish an upper limit of $r < 0.001$ with 95% confidence level in the absence of a detection. LiteBIRD (Light satellite for the studies of B-mode polarization and Inflation from cosmic background Radiation Detection) [81] is dedicated to achieving a measurement of r within an uncertainty of $\delta r = 10^{-3}$. Similarly, PICO (Probe of Inflation and Cosmic Origins) [82, 83] aims to detect $r = 5 \times 10^{-4}$ at a

²The standard non-minimal Higgs inflation model encounters an inconsistency [71–74] related to the validity of the effective field theory. This issue arises because achieving inflation with subplanckian field values $\phi \leq m_P$ requires large values of the coupling $c_{\mathcal{R}}$ (δ here). Consequently, the inflationary scale becomes larger than the Ultraviolet (UV) cut-off of the effective theory, causing the theory to break down above it. In the model studied here, however, the coupling function has the form $\simeq 1 + c_{\mathcal{R}}\phi^4$, and as shown in [75–77], there is no problem with unitarity.

significance level of 5σ . Additional missions include CORE (Cosmic Origins Explorer) [84], which is projected to exhibit sensitivity to r as low as 10^{-3} ; PIXIE (Primordial Inflation Explorer) [85], anticipates to measure $r < 10^{-3}$ at the 5σ level; and PRISM (Polarized Radiation Imaging and Spectroscopy Mission) [86], which aspires to achieve detection of r as low as 5×10^{-4} at 5σ . The large tensor modes ($r \sim 10^{-3}$) obtained in both models of smooth μ -hybrid inflation and non-minimal Higgs inflation are potentially measurable by these upcoming CMB experiments.

6 Proton Decay

In the G_{422} model, proton decay is mediated by color triplets in $F, F^c \supset d, d^c, H^c, \bar{H}^c \supset d_H^c, \bar{d}_H^c$, and $G \supset g, g^c$, rather than via gauge bosons [40]. These color triplets acquire superheavy masses from the following superpotential terms:

$$W \supset a G H^c H^c + b G \bar{H}^c \bar{H}^c \supset m_{d_H^c} g d_H^c + m_{\bar{d}_H^c} g^c \bar{d}_H^c, \quad (6.1)$$

where $m_{d_H^c} = aM$ and $m_{\bar{d}_H^c} = bM$. The $U(1)_R$ symmetry plays a vital role in forbidding undesirable baryon number-violating operators that can lead to fast proton decay. These include $d = 4, B$ and L violating operators such as:

$$\frac{F_i F_j F_k^c H^c}{m_P} \supset \frac{M}{m_P} (L_i L_j e_k^c + Q_i L_j d_k^c), \quad \frac{F_i^c F_j^c F_k^c H^c}{m_P} \supset \frac{M}{m_P} u_i^c d_j^c d_k^c, \quad (6.2)$$

which are invariant under the gauge symmetry G_{422} but not under the $U(1)_R$ symmetry. Similarly, some gauge invariant $d = 5$ proton decay operators can appear at the non-renormalizable level, such as:

$$\frac{F_i^c F_j^c F_k^c F_l^c}{m_P} \supset \frac{(u_i^c u_j^c d_k^c e_k^c + u_i^c d_j^c d_k^c \nu_k^c)}{m_P}, \quad \frac{F_i F_j F_k F_l}{m_P} \supset \frac{Q_i Q_j Q_k L_l}{m_P}, \quad (6.3)$$

but are also not allowed by the $U(1)_R$ symmetry. The proton decay rate via dimension-6 operators [40] with $M \simeq 2 \times 10^{17}$ GeV, $M_{\nu_i} \simeq 10^{14}$ GeV and natural values of the couplings $a, b \sim 1$, is heavily suppressed to have any observable signature in the next generation of experiments such as Hyper-Kamiokande [87], JUNO [88] and DUNE [89, 90].

7 Summary

We have implemented two inflationary models within the framework of $G_{422} \equiv SU(4)_C \times SU(2)_L \times SU(2)_R$ GUT gauge symmetry, including a smooth variant of μ -hybrid inflation and a non-minimal Higgs inflation model. Both effectively generate the MSSM μ -term, and since the G_{422} GUT gauge symmetry is spontaneously broken to SM gauge group

during inflation, the primordial magnetic monopoles are inflated away. Notably, both models exhibit a tree-level inclination, obviating the need for radiative corrections.

The smooth μ -hybrid model, with a minimal canonical Kähler potential and soft SUSY masses $m_{3/2} \simeq 100$ TeV, proves incompatible with experimental observations. However, a non-minimal Kähler potential enhances the parametric space, resulting in a scalar spectral index n_s that aligns perfectly with the central value of Planck2018 + BK15 data bounds.

The non-minimal Higgs model also predicts a scalar spectral index n_s that aligns very closely to the central observationally favored value of the Planck2018 + BK15 data bounds. In both models, the inflationary phase is followed by reheating, during which the inflaton decays into the lightest right-handed neutrino, leading to non-thermal leptogenesis through the subsequent decay of the right-handed neutrinos. Furthermore, both models yield large tensor modes r ($\sim 10^{-3}$), potentially measurable in the upcoming generation of CMB experiments.

Acknowledgments

The author extends gratitude to Mansoor Ur Rehman and Constantinos Pallis for their insightful discussions and careful review of the manuscript. Additionally, the author would like to thank the editor for their invaluable suggestions, which greatly enhanced the quality of the manuscript.

References

- [1] Y. Akrami, *et al.* (Planck), “Planck 2018 results. X. Constraints on inflation,” *Astron. Astrophys.* **641**, A10 (2020), [arXiv:1807.06211 \[astro-ph.CO\]](#).
- [2] Marc Kamionkowski and Ely D. Kovetz, “The Quest for B Modes from Inflationary Gravitational Waves,” *Ann. Rev. Astron. Astrophys.* **54**, 227–269 (2016), [arXiv:1510.06042 \[astro-ph.CO\]](#).
- [3] Uros Seljak, and Matias Zaldarriaga, “Signature of gravity waves in polarization of the microwave background,” *Phys. Rev. Lett.* **78**, 2054–2057 (1997), [arXiv:astro-ph/9609169](#).
- [4] Marc Kamionkowski, Arthur Kosowsky, and Albert Stebbins, “Statistics of cosmic microwave background polarization,” *Phys. Rev. D* **55**, 7368–7388 (1997), [arXiv:astro-ph/9611125](#).
- [5] Uros Seljak, “Measuring polarization in cosmic microwave background,” *Astrophys. J.* **482**, 6 (1997), [arXiv:astro-ph/9608131](#).
- [6] Daniel Baumann and Liam McAllister, “Inflation and String Theory,” *Cambridge Monographs on Mathematical Physics* (Cambridge University Press), [arXiv:1404.2601 \[hep-th\]](#).
- [7] G.R. Dvali, Q. Shafi and R.K. Schaefer, “Large scale structure and supersymmetric inflation without fine tuning,” *Phys. Rev. Lett.* **73**, 1886 (1994), [arXiv:hep-ph/9406319](#).

- [8] Andrei Linde and Antonio Riotto, “Hybrid inflation in supergravity,” *Phys. Rev. D* **56**, R1841(R) (1997), [arXiv:hep-ph/9703209](#).
- [9] V.N. Senoguz and Q. Shafi, “Testing supersymmetric grand unified models of inflation,” *Phys. Lett. B* **567**, 79 (2003), [arXiv:hep-ph/0305089](#).
- [10] V.N. Senoguz and Q. Shafi, “Reheat temperature in supersymmetric hybrid inflation models,” *Phys. Rev. D* **71**, 043514 (2005), [arXiv:hep-ph/0412102](#).
- [11] Edmund J. Copeland, Andrew R. Liddle, David H. Lyth, Ewan D. Stewart, and David Wands, “False vacuum inflation with Einstein gravity,” *Phys. Rev. D* **49**, 6410 (1994), [arXiv:astro-ph/9401011](#).
- [12] Wilfried Buchmuller, Laura Covi, David Delepine, “Inflation and supersymmetry breaking,” *Phys. Lett. B* **491**, 183 (2000), [arXiv:hep-ph/0006168](#).
- [13] Mansoor Ur Rehman, Qaisar Shafi, Joshua R. Wickman “Supersymmetric hybrid inflation redux,” *Phys. Lett. B* **683**, 191 (2010), [arXiv:0908.3896 \[hep-ph\]](#).
- [14] Mansoor Ur Rehman, Qaisar Shafi, Joshua R. Wickman “Minimal supersymmetric hybrid inflation, flipped $SU(5)$ and proton decay,” *Phys. Lett. B* **688**, 75 (2010), [arXiv:0912.4737 \[hep-ph\]](#).
- [15] R. Jeannerot, S. Khalil, G. Lazarides, “Leptogenesis in smooth hybrid inflation,” *Phys. Lett. B* **506**, 344 (2001), [arXiv:hep-ph/0103229](#).
- [16] Rachel Jeannerot, Shaaban Khalil, George Lazarides and Qaisar Shafi, “Inflation and monopoles in supersymmetric $SU(4)_C \times SU(2)_L \times SU(2)_R$,” *JHEP* **10** (2000) 012, [arXiv:hep-ph/0002151](#).
- [17] S. Khalil, M. U. Rehman, Q. Shafi, and E. A. Zaakouk, “Inflation in supersymmetric $SU(5)$,” *Phys. Rev. D* **83**, 063522 (2011), [arXiv:1010.3657 \[hep-ph\]](#).
- [18] Waqas Ahmed and Umer Zubair, “Radiative symmetry breaking, cosmic strings and observable gravity waves in $U(1)_R$ symmetric $SU(5) \times U(1)_X$,” *JCAP* **01** (2023) 019, [arXiv:2210.13059 \[hep-ph\]](#).
- [19] G. Lazarides and C. Panagiotakopoulos, “Smooth hybrid inflation,” *Phys. Rev. D* **52**, R559(R) (1995), [arXiv:hep-ph/9506325](#).
- [20] Mansoor Ur Rehman and Qaisar Shafi, “Simplified smooth inflation with observable gravity waves,” *Phys. Rev. D* **86**, 027301 (2012), [arXiv:1202.0011 \[hep-ph\]](#).
- [21] Mansoor Ur Rehman and Umer Zubair, “Simplified smooth hybrid inflation in supersymmetric $SU(5)$,” *Phys. Rev. D* **91**, 103523 (2015), [arXiv:1412.7619 \[hep-ph\]](#).
- [22] K.-I. Izawa and T. Yanagida, “Natural new inflation in broken supergravity,” *Phys. Lett. B* **393**, 331 (1997), [arXiv:hep-ph/9608359](#).
- [23] K.-I. Izawa, M. Kawasaki and T. Yanagida, “Dynamical tuning of the initial condition for new inflation in supergravity,” *Phys. Lett. B* **411**, 249 (1997), [arXiv:hep-ph/9707201](#).
- [24] Mansoor Ur Rehman, Mian Muhammad Azeem Abid and Amna Ejaz, “New inflation in supersymmetric $SU(5)$ and flipped $SU(5)$ GUT models,” *JCAP* **11** (2020) 019, [arXiv:1804.07619 \[hep-ph\]](#).

- [25] Niamat Ullah Khan, Nadir Ijaz, and Mansoor Ur Rehman, “New inflation in the waterfall region,” *Phys. Rev. D* **108**, 123545 (2023), [arXiv:2309.06953 \[hep-ph\]](#).
- [26] Mian Muhammad Azeem Abid, Maria Mehmood, Mansoor Ur Rehman, Qaisar Shafi, “Realistic inflation in no-scale $U(1)_R$ symmetric flipped $SU(5)$,” *JCAP* **10** (2021) 015, [arXiv:2107.05678 \[hep-ph\]](#).
- [27] C. Pallis and N. Toumbas, “Non-minimal Higgs inflation and non-thermal leptogenesis in a supersymmetric Pati-Salam model,” *JCAP* **12** (2011) 002, [arXiv:1108.1771 \[hep-ph\]](#).
- [28] Mureed Hussain and Rizwan Khalid, “Yukawa unification with light supersymmetric particles consistent with LHC constraints,” *Nucl. Phys. B* **942**, 30 (2019), [arXiv:1812.06012 \[hep-ph\]](#).
- [29] Ilia Gogoladze, Rizwan Khalid, and Qaisar Shafi, “Yukawa unification and neutralino dark matter in $SU(4)_C \times SU(2)_L \times SU(2)_R$,” *Phys. Rev. D* **79**, 115004 (2009), [arXiv:0903.5204 \[hep-ph\]](#).
- [30] Waqas Ahmed, Mohamed Belfkir, Salah Nasri, Shabbar Raza, and Umer Zubair, “LHC run 3, b - τ Yukawa unification, and dark matter implications in a SUSY 4-2-2 model,” *Phys. Rev. D* **108**, 015016 (2023), [arXiv:2301.00332 \[hep-ph\]](#).
- [31] Ilia Gogoladze, Rizwan Khalid, Shabbar Raza and Qaisar Shafi, “Higgs and sparticle spectroscopy with Gauge-Yukawa unification,” *JHEP* **06**, (2011) 117, [arXiv:1102.0013 \[hep-ph\]](#).
- [32] Ilia Gogoladze, Rizwan Khalid, Shabbar Raza and Qaisar Shafi, “ t - b - τ Yukawa unification for $\mu < 0$ with a sub-TeV sparticle spectrum,” *JHEP* **12**, (2010) 055, [arXiv:1008.2765 \[hep-ph\]](#).
- [33] Shabbar Raza, Qaisar Shafi, and Cem Salih Ün, “NLSP gluino and NLSP stop scenarios from b - τ Yukawa unification,” *Phys. Rev. D* **92**, 055010 (2015), [arXiv:1412.7672 \[hep-ph\]](#).
- [34] Ilia Gogoladze, Mansoor Ur Rehman, and Qaisar Shafi, “Amelioration of the little hierarchy problem in $SU(4)_C \times SU(2)_L \times SU(2)_R$,” *Phys. Rev. D* **80**, 105002 (2009), [arXiv:0907.0728 \[hep-ph\]](#).
- [35] G. Dvali, G. Lazarides, Q. Shafi, “ μ Problem and hybrid inflation in supersymmetric $SU(2)_L \times SU(2)_R \times U(1)_{B-L}$,” *Phys. Lett. B* **424**, 259 (1998), [arXiv:hep-ph/9710314](#).
- [36] George Lazarides, Mansoor Ur Rehman, Qaisar Shafi, and Fariha K. Vardag, “Shifted μ -hybrid inflation, gravitino dark matter, and observable gravity waves,” *Phys. Rev. D* **103**, 035033 (2021), [arXiv:2007.01474 \[hep-ph\]](#).
- [37] Adeela Afzal, Maria Mehmood, Mansoor Ur Rehman, Qaiser Shafi, “Supersymmetric hybrid inflation and metastable cosmic strings in $SU(4)_C \times SU(2)_L \times U(1)_R$,” [arXiv:2308.11410 \[hep-ph\]](#).
- [38] Muhammad Atif Masoud, Mansoor Ur Rehman, and Mian Muhammad Azeem Abid, “Nonminimal inflation in supersymmetric GUTs with $U(1)_R \times Z_n$ symmetry,” *Int. J. Mod. Phys. D* **28**, 16 (2019), [arXiv:1910.10519 \[hep-ph\]](#).
- [39] S. F. King and Q. Shafi, “Minimal supersymmetric $SU(4)_C \times SU(2)_L \times SU(2)_R$,” *Phys. Lett. B* **422** (1998) 135, [arXiv:hep-ph/9711288](#).

- [40] George Lazarides, Mansoor Ur Rehman and Qaisar Shafi, “Proton Decay in Supersymmetric $SU(4)_C \times SU(2)_L \times SU(2)_R$,” *JHEP* **10**, (2020) 085, [arXiv:2007.15317 \[hep-ph\]](#).
- [41] A.H. Chamseddine, R.L. Arnowitt, and P. Nath, “Locally supersymmetric grand unification,” *Phys. Rev. Lett.* **49**, 970 (1982).
- [42] A.D. Linde and A. Riotto, “Hybrid inflation in supergravity,” *Phys. Rev. D* **56**, R1841 (1997), [arXiv:hep-ph/9703209](#).
- [43] H.P. Nilles, “Supersymmetry, supergravity and particle physics,” *Phys. Rept.* **110** (1984) 1.
- [44] Mansoor ur Rehman, Vedat Nefer Senoguz and Qaisar Shafi, “Supersymmetric And Smooth Hybrid Inflation In The Light Of WMAP3,” *Phys. Rev. D* **75**, 043522 (2007), [arXiv:hep-ph/0612023](#).
- [45] Wilfried Buchmüller, Valerie Domcke, Kohei Kamada and Kai Schmitz, “Hybrid Inflation in the Complex Plane,” *JCAP* **07**, 054 (2014), [arXiv:1404.1832 \[hep-ph\]](#).
- [46] V. N. Senoguz and Q. Shafi, “GUT Scale Inflation, Non-Thermal Leptogenesis, and Atmospheric Neutrino Oscillations,” *Phys. Lett. B* **582**, 6-14 (2004), [arXiv:hep-ph/0309134](#).
- [47] G. Lazarides and Q. Shafi, “Origin of matter in the inflationary cosmology,” *Phys. Lett. B* **258**, 305 (1991).
- [48] G. Lazarides, R. K. Schaefer, and Q. Shafi, “Supersymmetric inflation with constraints on superheavy neutrino masses,” *Phys. Rev. D* **56**, 1324 (1997), [arXiv:hep-ph/9608256](#).
- [49] G. Lazarides and N. D. Vlachos, “Atmospheric neutrino anomaly and supersymmetric inflation,” *Phys. Lett. B* **441**, 46 (1998), [arXiv:hep-ph/9807253](#).
- [50] Andrew R. Liddle and Samuel M. Leach, “How long before the end of inflation were observable perturbations produced?,” *Phys. Rev. D* **68**, 103503 (2003), [arXiv:astro-ph/0305263](#).
- [51] M. Fukugita and T. Yanagida, “Baryogenesis without grand unification,” *Phys. Lett. B* **174**, 45 (1986).
- [52] V.A. Kuzmin, V.A. Rubakov and M.E. Shaposhnikov, “On anomalous electroweak baryon-number non-conservation in the early universe,” *Phys. Lett. B* **155**, 36 (1985).
- [53] S.Yu. Khlebnikov and M.E. Shaposhnikov, “The statistical theory of anomalous fermion number non-conservation,” *Nucl. Phys. B* **308**, 885 (1988).
- [54] P. A. Zyla, *et al.* (Particle Data Group), “Review of Particle Physics,” *PTEP* **2020** (8), 083C01 (2020).
- [55] Markus A. Luty, “Baryogenesis via leptogenesis,” *Phys. Rev. D* **45**, 455 (1992).
- [56] Laura Covi, Esteban Roulet and Francesco Vissani, “CP violating decays in leptogenesis scenarios,” *Phys. Lett. B* **384** (1996) 169, [arXiv:hep-ph/9605319](#).
- [57] Johm Ellis, Jihn E. Kim and D.V. Nanopoulos, “Cosmological gravitino regeneration and decay,” *Phys. Lett. B* **145**, 181 (1984).
- [58] M.Yu. Khlopov and A.D. Linde, “Is it easy to save the gravitino?,” *Phys. Lett. B* **138**, 265 (1984).

- [59] Nadir Ijaz and Mansoor Ur Rehman, “Exploring Primordial Black Holes and Gravitational Waves with R-Symmetric GUT Higgs Inflation,” [arXiv:2402.13924 \[astro-ph.CO\]](#).
- [60] Nadir Ijaz, Maria Mehmood and Mansoor Ur Rehman, “The Stochastic Gravitational-Wave Background from Primordial Black Holes in R-Symmetric $SU(5)$ Inflation,” [arXiv:2308.14908 \[astro-ph.CO\]](#).
- [61] John Ellis, Dimitri V. Nanopoulos, and Keith A. Olive, “No-Scale Supergravity Realization of the Starobinsky Model of Inflation,” *Phys. Rev. Lett.* **111**, 111301 (2013), [arXiv:1305.1247 \[hep-th\]](#).
- [62] John Ellis, Dimitri V. Nanopoulos, and Keith A. Olive, “Starobinsky-like inflationary models as avatars of no-scale supergravity,” *JCAP* **10** (2013) 009, [arXiv:1307.3537 \[hep-th\]](#).
- [63] Michele Cicoli, Senarath de Alwis and Alexander Westphal, “Heterotic moduli stabilisation,” *JHEP* **10** (2013) 199, [arXiv:1304.1809 \[hep-th\]](#).
- [64] Hyun Min Lee, “Chaotic inflation in Jordan frame supergravity,” *JCAP* **08** (2010) 003, [arXiv:1005.2735 \[hep-ph\]](#).
- [65] Sergio Ferrara, Renata Kallosh, Andrei Linde, “Cosmology with Nilpotent Superfields,” *JHEP* **10** (2014) 143, [arXiv:1408.4096 \[hep-th\]](#).
- [66] C. Pallis and N. Toumbas, “Starobinsky-type inflation with products of Kähler manifolds,” *JCAP* **05** (2016) 015, [arXiv:1512.05657 \[hep-ph\]](#).
- [67] Constantinos Pallis, “Gravitational Waves, μ Term and Leptogenesis from $B - L$ Higgs Inflation in Supergravity,” *Universe* **2018**, 4(1), 13, [arXiv:1710.05759 \[hep-ph\]](#).
- [68] S.P. Martin, “A Supersymmetry Primer,” *Adv. Ser. Direct. High Energy Phys.* **21**, 1 (2010), [arXiv:hep-ph/9709356](#).
- [69] Motoi Endo, Masahiro Kawasaki, Fuminobu Takahashi and T. T. Yanagida, “Inflaton Decay through Supergravity Effects,” *Phys. Lett. B* **642**, 518-524 (2006), [arXiv:hep-ph/0607170](#).
- [70] Motoi Endo, Fuminobu Takahashi and T. T. Yanagida, “Inflaton Decay in Supergravity,” *Phys. Rev. D* **76**, 083509 (2007), [arXiv:0706.0986 \[hep-ph\]](#).
- [71] Alex Kehagias, Azadeh Moradinezhad Dizgah and Antonio Riotto, “Remarks on the Starobinsky model of inflation and its descendants,” *Phys. Rev. D* **89**, 043527 (2014), [arXiv:1312.1155 \[hep-th\]](#).
- [72] J. L. F. Barbón and J. R. Espinosa, “On the Naturalness of Higgs inflation,” *Phys. Rev. D* **79**, 081302 (2009), [arXiv:0903.0355 \[hep-ph\]](#).
- [73] C.P. Burgess, Hyun Min Lee and Michael Trott, “On Higgs inflation and naturalness,” *JHEP* **07** (2010) 007, [arXiv:1002.2730 \[hep-ph\]](#).
- [74] F. Bezrukov, A. Magnin, M. Shaposhnikov and S. Sibiryakov, “Higgs inflation: consistency and generalisations,” *JHEP* **01** (2011) 016, [arXiv:1008.5157 \[hep-ph\]](#).
- [75] Constantinos Pallis, “Unitarizing non-minimal inflation via a linear contribution to the frame function,” *Phys. Lett. B* **789**, 243 (2019), [arXiv:1809.10667 \[hep-ph\]](#).
- [76] Constantinos Pallis and Qaisar Shafi, “Gravity waves from non-minimal quadratic inflation,” *JCAP* **03** (2015) 023, [arXiv:1412.3757 \[hep-ph\]](#).

- [77] Constantinos Pallis, “Unitarity-safe models of non-minimal inflation in supergravity,” *Eur. Phys. J. C* **78**, 1014 (2018), [arXiv:1807.01154 \[hep-ph\]](#).
- [78] P. Ade *et al.* (Simons Observatory), “The Simons Observatory: Science goals and forecasts,” *JCAP* **02**, 056 (2019), [arXiv:1808.07445 \[astro-ph.CO\]](#).
- [79] K. Abazajian, G. Addison, P. Adshead, *et al.* (CMB-S4), “CMB-S4: Forecasting Constraints on Primordial Gravitational Waves,” *Astrophys. J.* **926**, 54 (2022), [arXiv:2008.12619 \[astro-ph.CO\]](#).
- [80] Sebastian Belkner, Julien Carron, Louis Legrand, *et al.* (CMB-S4), “CMB-S4: Iterative internal delensing and r constraints,” [arXiv:2310.06729 \[astro-ph.CO\]](#).
- [81] E. Allys *et al.* (LiteBIRD), “Probing Cosmic Inflation with the LiteBIRD Cosmic Microwave Background Polarization Survey,” *PTEP* **2023** (4), 042F01 (2022), [arXiv:2202.02773 \[astro-ph.IM\]](#).
- [82] Ragnhild Aurlen, *et al.* (PICO), “Foreground separation and constraints on primordial gravitational waves with the PICO space mission,” *JCAP* **06** (2023) 034, [arXiv:2211.14342 \[astro-ph.CO\]](#).
- [83] Shaul Hanany, *et al.* (PICO), “PICO: Probe of Inflation and Cosmic Origins,” [arXiv:1902.10541 \[astro-ph.IM\]](#).
- [84] F. Finelli, *et al.* (CORE), “Exploring cosmic origins with CORE: Inflation,” *JCAP* **04**, 016 (2018), [arXiv:1612.08270 \[astro-ph.CO\]](#).
- [85] A. Kogut, D. J. Fixsen, D. T. Chuss *et al.* (PIXIE), “The Primordial Inflation Explorer (PIXIE): A Nulling Polarimeter for Cosmic Microwave Background Observations,” *JCAP* **07**, 025 (2011), [arXiv:1105.2044 \[astro-ph.CO\]](#).
- [86] P. Andre *et al.* (PRISM), “PRISM (Polarized Radiation Imaging and Spectroscopy Mission): An Extended White Paper,” *JCAP* **02**, 006 (2014), [arXiv:1310.1554 \[astro-ph.CO\]](#).
- [87] K. Abe *et al.* (Hyper-Kamiokande Collaboration), “Hyper-Kamiokande Design Report,” [arXiv:1805.04163 \[physics.ins-det\]](#).
- [88] Fengpeng An *et al.* (JUNO Collaboration), “Neutrino Physics with JUNO,” *J. Phys. G: Nucl. Part. Phys.* **43**, 030401 (2016), [arXiv:1507.05613 \[physics.ins-det\]](#).
- [89] R. Acciarri *et al.* (DUNE Collaboration), “Long-Baseline Neutrino Facility (LBNF) and Deep Underground Neutrino Experiment (DUNE) Conceptual Design Report Volume 2: The Physics Program for DUNE at LBNF,” [arXiv:1512.06148 \[physics.ins-det\]](#).
- [90] B. Abi *et al.* (DUNE Collaboration), “Deep Underground Neutrino Experiment (DUNE), Far Detector Technical Design Report, Volume II: DUNE Physics,” [arXiv:2002.03005 \[hep-ex\]](#).